



Coral conglomerate platforms as foundations for low-lying, reef islands in the French Polynesia (central south Pacific): New insights into the timing and mode of formation

Lucien F. Montaggioni, Bertrand Martin-Garin, Bernard Salvat, Annie Aubanel, Edwige Pons-Branchu, Martine Paterne, Mailys Richard

► To cite this version:

Lucien F. Montaggioni, Bertrand Martin-Garin, Bernard Salvat, Annie Aubanel, Edwige Pons-Branchu, et al.. Coral conglomerate platforms as foundations for low-lying, reef islands in the French Polynesia (central south Pacific): New insights into the timing and mode of formation. *Marine Geology*, 2021, 437, pp.106500. 10.1016/j.margeo.2021.106500 . hal-03233484

HAL Id: hal-03233484

<https://hal.science/hal-03233484>

Submitted on 24 May 2023

HAL is a multi-disciplinary open access archive for the deposit and dissemination of scientific research documents, whether they are published or not. The documents may come from teaching and research institutions in France or abroad, or from public or private research centers.

L'archive ouverte pluridisciplinaire **HAL**, est destinée au dépôt et à la diffusion de documents scientifiques de niveau recherche, publiés ou non, émanant des établissements d'enseignement et de recherche français ou étrangers, des laboratoires publics ou privés.



Distributed under a Creative Commons Attribution - NonCommercial 4.0 International License

1 Coral conglomerate platforms as foundations for
2 low-lying, reef islands in the French Polynesia
3 (central south Pacific): new insights into the timing
4 and mode of formation

5 Lucien F. Montaggioni^a, Bertrand Martin-Garin^a,
6 Bernard Salvat^b, Annie Aubanel^c, Edwige Pons-
7 Branchu^d, Martine Paterne^d, Mailys Richard^d

8 ^a Aix Marseille Univ, CNRS, IRD, Coll France, INRAE, CEREGE, 13331
9 Marseille, France

10 ^b PSL-École pratique des hautes études, USR3278, EPHE, CNRS, UPVD,
11 CRIOBE, Labex Corail, université de Perpignan, 66860 Perpignan, France

12 ^c Environmental Consultant, BP 2038 Papeete, 98713 Tahiti, Polynésie
13 Française

14 ^d LSCE/IPSIL, CEA-CNRS-UVSQ, Université Paris-Saclay, 91198 Gif-sur-
15 Yvette, France

16 Corresponding author, Email address: montaggioni@cerege.fr

17 Highlights

- 18 – In the French Polynesia, reef conglomerate platforms**
19 accreted mainly between 3,000 and 1,000 yr BP.
- 20 – Conglomerate-clast deposition and lithification**
21 occurred relatively synchronously.
- 22 – From 2,500 to 1,000 yr BP, accretion of conglomerates**
23 and overlying atoll-rim islands interplayed from lagoon
24 borders seawards.

25 Abstract

26 In French Polynesia, low-lying, reef islands, composed of
27 unconsolidated skeletal material rest on cemented
28 conglomerate platforms. These are regarded as mainly
29 generated by storm activity during the mid-late Holocene. Field
30 observations and coral sampling were carried out on
31 conglomerates from three atolls located in the north-western
32 Tuamotu, namely, Takapoto, Takaroa and Fakarava. There,
33 fifty-seven samples were dated using the uranium-thorium
34 (U/Th) method. The lateral age distribution of clasts indicates
35 that conglomerate platforms have accreted from lagoon sides
36 seawards

37 In addition to U/Th dating, the coral clast-age datasets include
38 eighteen calibrated radiocarbon ages from Takapoto and other
39 Tuamotu atolls – Takapoto, Mataiva, Rangiroa, Arutua,
40 Apataki, Marokau, Hao, Pukarua, Nukutavake. As a matter of
41 comparison, another seventy-seven, previously published
42 radiometric conglomerate ages from various French Polynesian
43 islands (Society, Tuamotu, Gambier) were incorporated in the
44 present study. It appears that formation of conglomerate
45 platforms has taken place principally during a 2,000-year
46 interval, between 3,000 and 1,000 yr BP when sea level
47 dropped from about 0.60 m to its present position. Before and
48 after these periods, lower amounts of coral detritus have been
49 provided to conglomerates, possibly due to clast deposition in

50 adjacent lagoons and to trapping into reef rim-islands
51 respectively.

52 Age discrepancies of most coral clasts collected from multiple
53 stacked layers at Takapoto and Fakarava do not exceed 500
54 years, strongly suggesting limited clast reworking before final
55 stabilization. The superimposition of two to four firmly
56 cemented conglomeratic layers at the same place gives
57 evidence that marine cementation has operated shortly after
58 clast deposition. This event is regarded as having taken place
59 within both phreatic and vadose environments. Rubble sheets
60 found seawards at some atoll-rim sites are interpreted to be
61 conglomerates in the making, emplaced over the last centuries.

62 Dating of atoll-islet material indicates clearly that, over the
63 2,500–1,000 yr-BP span, the building of conglomerates and
64 overlying islets has interplayed. The former have evolved
65 within subtidal to supratidal zones while the latter have been
66 accreted subaerially. This may explain the firmly consolidated
67 state of platforms and the unconsolidated state of islets. Due to
68 their firmness, conglomerate platforms are assumed to be key
69 structures for the maintenance of atoll islands subjected to sea
70 level rise and increasing storminess in the coming centuries.

71 **Keywords**

72 Atolls

73 Conglomerate platforms

74 Marine cementation

75 Mid-late Holocene

76 Tuamotu
77 French Polynesia.

78 **1 Introduction**

79 Accelerated sea-level rise and increasing storm intensity as
80 natural responses to current anthropogenic global warming are
81 usually thought to generate marked changes in coastal
82 hydrodynamic regimes and sediment transport over the coming
83 centuries (IPCC, 2019; Bramante et al., 2020). At the end of the
84 21st century, according to Representative Concentration
85 Pathway (RCP) 8.5, eustatic sea-level rise could surpass the
86 present level by about 2 m (Kopp et al., 2014, 2017; Slangen et
87 al., 2014; Le Bars et al., 2017; Horton et al., 2020) while
88 storms and cyclones are expected to significantly increase in
89 intensity (Bhatia et al., 2018; Holland et al., 2019; Liu et al.,
90 2019) and as such to create stronger storm surges (Lin et al.,
91 2013). These effects will get worse in the tropical regions,
92 where sea level will exceed the global average (Becker et al.,
93 2012; Botella, 2015) and cyclone intensity is known to have
94 risen over the last decades (Emanuel, 2007; Knutson et al.,
95 2010; Kossin et al., 2020). For instance, 20% increase in
96 maximum cyclonic winds result in 30 to 100% increase in
97 surge and inundation along the coastline and the flooding
98 penetrates deep inland (Lin et al., 2019). Such events can cause
99 broad-scale disturbances on coral reefs. As a whole, there are
100 extensive mortality of hard corals and increasing dominance of

101 algae and soft corals over hard corals (Cheal et al., 2017;
102 Vercelloni et al., 2019; Puotinen et al., 2020). Projections
103 suggest that sea level will rise by at least 2 m over the coming
104 centuries to millennia (Clark et al., 2016; IPCC, 2019).
105 Moreover, the tropical Pacific exhibits numerous atolls, i.e.
106 low-lying coral reef islands. Their upper rim surfaces exhibit
107 more or less continuous accumulations of thin landmasses that
108 form islets – *motu* in the Polynesian language. These islets are
109 composed of unconsolidated, reef-derived detritus, mainly
110 coral pebbles to skeletal sands, reaching up to a maximum
111 elevation of about 4 m above mean tide levels. Islets are locally
112 separated by shallow channels – *hoa* in the Polynesian
113 language – usually shoaling at low tide (McLean, 2011a;
114 Woodroffe and Biribo, 2011). As a result of the balance
115 between destructive wave forces and constructive reef-derived
116 supply, the islets are known to be periodically reshaped by
117 cyclonic events (Stoddart, 1985; Scoffin, 1993; Harmelin-
118 Vivien, 1994). Due to ongoing climate change, the fate of
119 moving islets by the end of the 21st century remains uncertain.
120 Observations, projections and modelling aiming at tentatively
121 explaining their dynamic behaviour are controversial. Different
122 evolutionary scenarios have been proposed: island stability
123 (Webb and Kench, 2010; Pala, 2014; Kench et al., 2015;
124 McLean and Kench, 2015; Beetham et al., 2017; Duvat et al.,
125 2017; East et al., 2020), island accretion (Kench et al., 2014a;

126 Stanley, 2019; Masselink et al., 2020) or erosion and flooding
127 (Van Dongeren et al., 2013; Hubbard et al., 2014; Shope et al.,
128 2016; Vitousek et al., 2017; Storlazzi et al., 2011, 2018). While
129 the dynamic responses of atoll islets to increasing natural
130 disturbances remain uncertain, the only sure source of stability
131 relates to cemented conglomerate platforms over which islets
132 have settled.

133 Also called conglomerate pavements and promenades, rampart
134 rocks, benches, shingle and boulder conglomerates or eustatic
135 terraces, these platforms are defined as emergent, usually
136 horizontal to sub-horizontal, flat-topped beds, composed of
137 weakly to firmly lithified, reef-derived carbonate material,
138 principally composed of coral gravels and pebbles, about
139 0.50 m to 2 m thick in areas subject to microtidal regimes. They
140 remained generally exposed above present high tide level. Such
141 features were believed to have been generated by storms and
142 cyclones (Newell and Bloom, 1970; Kench et al., 2014b;
143 Scoffin and McLean, 1978; McLean, 2011b; Montaggioni,
144 2011). As such, they occur mainly along the windward atoll
145 rims, but are occasionally present on leeward coasts. Their
146 planar topography was sometimes interpreted as resulting from
147 marine abrasion; a primary, depositional origin is now favoured
148 as they are recognised to be the cemented counterparts of
149 rubble sheets that accumulate today on reef flats close to sea
150 level (McLean, 2011b; Montaggioni, 2011).

151 These platforms are common features on Indo-Pacific atolls
152 (Woodroffe et al., 1999 for review). Similar reef conglomerates
153 are also found on continental shelf- and island-barrier-reefs
154 (Australian Great Barrier Reef: Scoffin and McLean, 1978;
155 French Polynesia, Society Islands: Pirazzoli, 1985, Hallmann et
156 al., 2020; Gambier Islands: Hallmann et al., 2020).
157 Radiometric dating of individual coral clasts extracted from
158 conglomerate platforms indicate that deposition occurred
159 between 6,000 and less than 1,000 yr BP (Pirazzoli, 1985;
160 Scoffin et al., 1985; Pirazzoli and Montaggioni, 1986, 1988;
161 Woodroffe et al., 1999; Montaggioni et al., 2018, 2019a;
162 Hallmann et al., 2020).
163 Based on radiometric ages of coral clasts, the present paper
164 aims at revisiting the timing and mode of formation of
165 conglomerate platforms in a number of the French Polynesia
166 islands (central south Pacific), with special reference to
167 Takapoto, Takaroa and Fakarava Atolls, in the Tuamotu
168 archipelago.

169 **2 Environmental setting**

170 *2.1 Location of study areas*

171 French Polynesia lies in the south-central Pacific from 7°50'S
172 to 27°00'S and from 134°28'W to 154°40'W, and occupied a
173 total area of about 5 500 000 km². This is composed of five
174 distinct archipelagoes, namely the Society, the Tuamotu, the

175 Marquesas, the Austral, and the Gambier. The Society island
 176 group comprises reef-bearing, high volcanic islands – Tahiti-
 177 Nui, Tahiti-Iti, Moorea, Raiatea, Tahaa, Huahine, Bora Bora,
 178 Maupiti – and a few atolls including Tupai, Scilly. The
 179 Tuamotu islands are strictly of atoll types. The Austral group
 180 exhibits volcanic islands surrounded by coral reefs, including
 181 Tubuai. The Gambier group consists of volcanic high islets –
 182 including Mangareva, Aukena, Akamaru – enclosed within a
 183 fringing-reef system and the atoll of Temoe. The Marquesas are
 184 devoid of coral reefs at sea level.

185 The Tuamotu Archipelago extends over 1500 km long and 500
 186 km wide. The average depth of the submarine plateau upon
 187 which the islands rise, does not exceed –2000 m (Fig. 1). The
 188 three atolls under study are located in the northwestern part of
 189 the archipelago. Takapoto Atoll lies between 14°37'39"S and
 190 145°12'18"W (Fig. 2a). It is 17 km long and 5.5 km wide. Its
 191 total emerged land area is 23 km². The rim is 300 to 400 m
 192 wide, almost continuously covered by islets directly lying on
 193 conglomerate platforms. The rim enclosed a lagoon, 78.64 km²
 194 in total area and approximately 43 m in maximum depth
 195 (Andréfouët et al., 2020). Takaroa Atoll is located 10 km
 196 northeast of Takapoto, at 14°27'00"S and 144°58'59"W. It is
 197 27.4 km long and 6.7 km wide (Fig. 2b). The emerged total
 198 land rim area is 20 km². The lagoon is 85.96 km² in surface
 199 area and 48 m in maximum depth (Andréfouët et al., 2020) and

200 displays only one pass, about 3 m deep, at the western rim side.

201 Fakarava Atoll is located at 16°18' S and 145°36'W. It is

202 rectangular-shaped, 54.9 km long and 24.9 km in maximum

203 width. It is an open atoll, with two asymmetric reef rims. The

204 largest, western rim side is about 500 m wide, devoid of sub-

205 aerial islets and frequently submerged at high tide (Fig. 2c).

206 The eastern rim side is approximately 150–180 m wide and

207 occupied by an almost continuous island lying on large

208 conglomerate pavements. The total land area of the emergent

209 rim is 27 km² (Duvat et al., 2020). The lagoon is one of the

210 deepest in the Tuamotu, with a maximum depth of about 60 m,

211 and studded with numerous reef patches in its western part,

212 locally capped by conglomerate terraces, unconsolidated rubble

213 spreads and dense vegetation.

214 The outer part of the atoll rims refers to a living coral-reef

215 system, subdivided into three zones – reef-flat, upper forereef

216 and lower forereef zones – from the shoreline seawards

217 (Chevalier et al., 1979; Salvat, 1981; Delesalle, 1985; Gabrié

218 and Salvat, 1985; Salvat and Richard, 1985). The reef-flat zone

219 is a subhorizontal surface, not exceeding –0.50 m deep at

220 spring low tide, and ranges from about 50 m to 200 m in width.

221 Coral cover rate of reef-flat areas averages generally less than

222 5 % of the total surface, but increases seawards close to the reef

223 front as does coralline algal coverage. The upper forereef zone

224 is composed of a gently dipping (< 20°) spur-and-groove

225 system, extending downwards to about –3 m to –10 m. Upper
226 foreef zones are mostly covered by pocilloporids showing
227 higher coral cover rate, up to 20 %. The lower forereef zone
228 comprises low-gradient to sub-vertical slopes to depths greater
229 than –60 m, with a series of terraces at mid-depths depending
230 on locations. Along lower forereef slopes and terraces, coral
231 coverage increases markedly from 30 % to up to 80 %, with a
232 growing dominance of poritids (Bouchon 1983; Faure and
233 Laboute, 1984; Delesalle, 1985; Kühman and Chevalier, 1986;
234 Montaggioni et al., 2019b).

235 2.2 *Climate and natural hazard events*

236 In the French Polynesia, the climate is tropical, warm and
237 humid. In the region, it is influenced by both the trade winds
238 blowing from northeast and southeast sectors and tropical and
239 extratropical storms (Andréfoüet et al., 2012). The rainy, hot
240 season (austral summer) extends from November to March.
241 The dryer, cooler austral winter is from April to October.
242 Annual rainfall ranges between 1,200 and 2,500 mm along a
243 northwest–southeast gradient. Monthly air temperatures
244 average 23–28 °C. Seawater temperatures vary from 26 °C to
245 30 °C, but decrease gradually southwards and eastwards. The
246 Tuamotu atolls frequently received warmer waters coming
247 from the equatorial belt and, as a result, during the winter, sea
248 surface temperatures do not drop below 22 °C. The eastward

249 migration of warmer waters during ENSO events favors the
250 motion of tropical storms further east into the Tuamotu region
251 (Larrue and Chiron, 2010).

252 The dominant trade winds are active throughout the year.
253 However, in summer times, from April to June, there are calm
254 periods with wind rates of less than 1 m/s. By contrast, during
255 the austral winter, gusts from the southeast are blowing at rates
256 of 10–15 m/s.

257 Tropical cyclones come usually from the northeast and
258 northwest sectors, between November and April. However, the
259 region is rarely affected by cyclone impacts. In northern
260 Tuamotu, the cyclone frequency is one to three per century, but
261 increases from four to eight per century towards the southeast
262 (Gabri   and Salvat, 1985). Cyclones may generate storm surges
263 as high as 8 m to 10 m. Waves higher than 12 m are revealed to
264 have a 50-year return period (Canavesio, 2014). Contrary to
265 Takaroa and Takapoto, during the austral summer, Fakarava is
266 partly protected from wave surges coming from the remote
267 northern sources owing to the *atoll shadow effect* provided by
268 atolls located further north (Andr  fo  et et al., 2012). During
269 the austral winter, the combination of strong trade winds and
270 southern distant-source swells result in stronger hydrodynamic
271 conditions in western Tuamotu. Due to its location at the
272 western border of the Tuamotu Archipelago, Fakarava is

273 severely impacted by waves generated from the southern and
 274 southwestern sectors, contrary to Takapoto and Takaroa.
 275 There are five swell regimes in the considered region. The three
 276 dominant regimes are driven by the trade-winds. The last two
 277 swell regimes originated from the northern and western sectors,
 278 both related to tropical depressions, are less frequent (Gabrié
 279 and Salvat, 1985). During the austral summer, swell heights do
 280 not exceed 2 m on average. During the austral winter, swells
 281 approximate 2.5 m high, but can occasionally exceed 4 m high
 282 (Andréfouët et al., 2012).
 283 Tides are semi-diurnal. The tidal amplitude around Tahiti and
 284 the north-west Tuamotu islands ranges from 0.20 m to 0.50 m
 285 at spring tide and about 0.10 m to 0.25 m at neap tide (Bongers
 286 and Wyrski, 1987; Pagès et al., 2001; Hallman et al., 2020).
 287 The present mean sea-level datum (pmsl) ranges between 0.20–
 288 0.25 m above the mean low water spring level (Pagès et al.,
 289 2001). In the fossil record, this level can be estimated using the
 290 elevation reached by the upper surfaces of emerged micro-
 291 atolls (Pirazzoli and Montaggioni, 1986; Woodroffe and
 292 McLean, 1990; Hallmann et al., 2018, 2020). In the northern
 293 Tuamotu, satellite altimetry indicates global sea level rise at
 294 rates of 2.4 mm/yr or more (Becker et al., 2012), higher than
 295 those of the global rise (1.2 ± 0.2 mm/yr; Hay et al., 2015).
 296 Little is known about the frequency and amplitude of storm
 297 surges generated by earthquake-generated tsunamis. According

298 to Etienne (2012) and Lau et al. (2016), available historical
299 records indicate that, since the 16th century, the Tuamotu has
300 suffered less than ten tsunami events, generating wave surges
301 of 0.3 m to 1.9 m high. The low frequency and magnitude of
302 tsunamis in the Tuamotu is confirmed by current observations
303 and numerical modeling (Sladen et al., 2007). In addition,
304 unusually high swell surges could be triggered by flank
305 collapses of volcanic islands (Clouard and Bonneville, 2003,
306 2004). Fracture networks and collapse-related scars were
307 described from the outer margins of a number of Tuamotu atoll
308 rims (Chevalier et al., 1968; Faure and Laboute, 1984;
309 Montaggioni et al., 2019b). Such wave surges could play a
310 significant role in occasionally supplying reef rims in skeletal
311 detritus from outer reef slopes.

312 **3 Materials and methods**

313 *3.1 Location of study sites and sample collection*

314 During the last three years (2017–2020), coral specimens for
315 dating were extracted from conglomerate platforms on
316 Takapoto, Takaroa and Fakarava Atolls, in the northwestern
317 Tuamotu (Table 1). Elevations of conglomerate surfaces and
318 locations of individual coral clasts to be dated were determined
319 using a conventional automatic level. Each reference point at
320 the top surface of a given conglomeratic bed and at the
321 sampling sites was positioned using DGPS coordinates.

322 Elevations were measured by reference to pmsl in each
323 considered site. Elevation uncertainties vary from island to
324 island and from site to site. Accordingly, elevations are given at
325 a maximum range of ± 0.30 m due to uncertainties in GPS
326 measurements, ellipsoid heights and altitude accuracy
327 (Hallmann et al., 2018, 2020).

328 At Takapoto Atoll, coral specimens come from three transects
329 perpendicular to the shoreline, respectively in the southeastern
330 and southwestern rim sides (Montaggioni et al., 2018, 2019a).
331 Additional samples were taken in the southeastern *hoa* system
332 (Figs. 4a, 5a), the northeastern rim side (Montaggioni et al.,
333 2018) (Fig. 4c) and from rubble sheets close to the
334 northwestern *hoa* area (courtesy of Samuel Etienne). (Figs. 4b,
335 5b).

336 At Takaroa, the selected site survey is located in the northeast
337 part of the atoll rim, on the edge of a *hoa* system (Fig. 6a, b)

338 At Fakarava, the study area is situated in the southeastern end
339 of the atoll (Fig. 7a, b, c, d). Additional specimens were
340 collected from conglomerates capping two lagoonal reef
341 patches referred to as Reef Patch A (Fig. 8a, b, c) and Reef
342 Patch E (Fig. 9a, b, c).

343 During the 1980s, coral clasts were collected from
344 conglomerate platforms in a number of Tuamotu atolls
345 (Pirazzoli and Montaggioni, 1984, 1986, 1988a,b; Montaggioni
346 and Pirazzoli, 1984; Pirazzoli, 1985; Pirazzoli et al., 1987) and

347 in the Society Island group (Pirazzoli, 1985; Montaggioni and
348 Pirazzoli, 1984; Pirazzoli and Montaggioni, 1988 for more
349 detailed information about field methods) (Table 1). As a
350 matter of comparison, previously published, U/Th-dated
351 conglomerate samples from other French Polynesian islands
352 were incorporated into the present database, taken from Moorea
353 (Rashid et al., 2014), Bora Bora, Moorea, Rangiroa, Tikehau,
354 Fakarava, Hao, Makemo and Gambier (Hallmann et al., 2020)
355 respectively (Table 1).

356 3.2 Radiometric dating procedures.

357 The coral samples from reef conglomerates in the Tuamotu and
358 Society islands (Table 1) formerly, dated by conventional
359 radiocarbon methods were calibrated (Tables 2 and 3) using the
360 IntCal Marine20 radiocarbon calibration (Heaton et al., 2020)
361 and the CALIB REV8.2 software (Stuiver and Reimer, 1993;
362 Stuiver et al., 2020). A mean value of ΔR of -140 ± 20 years
363 was applied from measured reservoir ages in French Polynesian
364 islands (Petchey et al., 2008). The relevant ages are expressed
365 in years BP (Before 1950).

366 Concerning samples dated using uranium-thorium dating
367 procedures, millimetric pieces of coral elements were cut using
368 a micro saw in order to select the most clean and pristine parts.
369 These pieces were rinsed with Milli-Q[®] water and
370 ultrasonicated several time. After adding a triple ^{229}Th ^{233}U –

371 ^{236}U spike in a Teflon beaker, samples – from ca 100 to
372 350 mg – were dissolved with diluted HCl. The U-Th
373 separation and purification were performed after
374 coprecipitation with $\text{Fe}(\text{OH})_3$, on 0.6 ml columns filled with U-
375 TEVA and pre-filter resins, in nitric media (see Pons-Branchu
376 et al., 2014 for technical details). The U and Th isotopic
377 compositions were analyzed at the *Laboratoire des sciences du*
378 *climat* (LSCE, France), on a Multi-Collector inductively coupled
379 plasma source mass spectrometer (MC-ICPMS) Thermo
380 ScientificTM Neptune^{Plus} fitted with a desolvating introduction
381 system (aridus II) and a jet interface. For mass fractionation
382 correction, we used an exponential mass fractionation law-
383 normalized to natural $^{238}\text{U}/^{235}\text{U}$ isotopic ratio and standard
384 sample bracketing. More details on the analytical procedure
385 (chemistry and MC-ICPMS analysis) can be found in Pons-
386 Branchu et al. (2014). After corrections for peak tailing,
387 hydrate interference and chemical blanks, $^{230}\text{Th}/^{234}\text{U}$ ages were
388 calculated (Table 2) from measured atomic ratios through
389 iterative age estimation using the ^{230}Th , ^{234}U and ^{238}U decay
390 constants of Cheng et al. (2013) and Jaffey et al. (1971). In
391 order to compare recalibrated radiocarbon and U/Th ages, the
392 latter, usually expressed in calendar years before the year of
393 measurement (2018, 2019 or 2020) were re-calculated to be
394 given in years before 1950 (**Supplementary material**).

395 **4 Results**

396 *4.1 Gross morphology of conglomerate platforms in the* 397 *Tuamotu*

398 In the study Tuamotu areas, conglomerate platforms occur as
399 weakly to firmly cemented flagstones, usually extending from
400 the outer- to inner-rim sides (Figs. 6a, 7a, 8a). This suggests
401 that conglomerates usually form almost continuous veneers
402 beneath atoll rim-islets (Figs. 3a, b, 4c). Every outcrop extends
403 from a few tens to several thousand square metres. Although a
404 given conglomeratic bed can vary in thickness by a few tens of
405 centimetres laterally, it usually has a relatively fairly constant
406 elevation. The thickness of the platforms is found to vary from
407 atoll to atoll, between 0.50 m and about 1.50 m. The thickest
408 conglomeratic platforms are encountered on the surface of
409 lagoonal coral patches at Fakarava where they reach up to 1 m
410 in height. The sediments are poorly sorted, rudstones to
411 floatstones. The larger, gravel- to pebble-sized clasts consist
412 mostly of corals (pocilloporids dominating), with low amount
413 of molluscan shells. The finer, sand-grained fraction is
414 composed of a variety of skeletal components (foraminifera
415 dominating) serving as matrices for larger detritus. Locally, the
416 platforms can be made up of one single to four superimposed
417 distinct rubble layers, separated by bedding planes (Figs. 5a,

418 7c, 7b, 7d, 9b, 9c). The exposures are locally undercut by
419 erosional notches close to pmsl (Figs. 7c, 9c).

420 4.2 Age distribution of conglomerate clasts

421 Calibrated radiocarbon and uranium-thorium ages of coral
422 clasts from the studied conglomerate platforms in the Tuamotu
423 range from about 6,600 yr BP to less than 400 yr BP. There
424 seems to be similar patterns of age distribution throughout the
425 Tuamotu islands. On the basis of the fifty-three conglomerate-
426 clast samples from Takapoto, Takaroa and Fakarava, 30.1 % of
427 the ages range between 2,000 and 1,000 yr BP, 54.7 % between
428 3,000 and 1,000 yr BP and 74.6 % between 4,000 and 1,000 yr
429 BP (Fig. 10a). By adding the calibrated ^{14}C results from other
430 conglomerate clasts in Takapoto, Mataiva, Rangiroa, Arutua,
431 Apataki, Hao, Pukarua and Nukutavake Atolls, a similar pattern
432 emerges. Out of a total of 75 dated samples, 39.4 % of the ages
433 are clustered between 2,000 and 1,000 yr BP, 58 % between
434 3,000 and 1,000 yr BP and 72.8 % between 4,000 and 1,000 yr
435 BP (Fig. 10b).

436 4.3 Lateral age distribution of clasts

437 The age distribution pattern of clasts trapped into conglomerate
438 platforms gives evidence of an increasing age trend from the
439 outer shoreline lagoonwards across atoll rims (Fig. 11). Thus,
440 at Takapoto, conglomeratic clasts (BAT 83, 85, 86; SAT 87A,
441 SAT 102 to SAT 109) close to the seaward side yielded ages of

about 1,400 to 3,300 yr BP while ages of the innermost coral debris (BAT 56, 103, 104; SAT 37A, 97A, 101A) range from around 2,250 to 6,500 yr BP. Similarly, at Takaroa, along the tested 227-m wide, conglomerate platform, clast ages tend to increase regularly from about 1,200 yr BP (SAT 149) to 2,500 yr BP (SAT 158) with few age inversions (Fig. 6a). A similar trend is observed on Fakarava where conglomeratic detritus (FAK 26, 27, 28) located less than 50 m behind the reef front line provided ages of 3,630–5,300 yr BP. By contrast, most of those (FAK 31, 32, 60) deposited up to 200 m landwards range in age from around 5,400 to 6,250 yr BP (Fig. 7a, b, c).

4.4 Vertical age distribution of clasts.

As indicated above, the thickness of conglomerate platforms varies from site to site, irrespective of exposition to swells. Platforms consisting of one-single bed do not exceed 0.30–0.50 m thick on average. By contrast, at Takapoto, along the southeastern rim side, the 1.20 m-thick pavement is composed of four superimposed individual beds (Fig. 5a). At Fakarava, the southeastern rim is covered by two-layer platforms, not exceeding 0.70–1 m in total thickness (Fig. 7b). Similarly, atop of the lagoonal reef patch E, conglomerates with 3 distinct layers, have accumulated on a thickness of 1.30 m (Fig. 9b, c). On other Tuamotu atolls and Society Islands, similar rock evidence has been described (Newell and Bloom, 1970;

466 Pirazzoli, 1985; Montaggioni and Pirazzoli, 1984;
 467 Montaggioni, pers.observ.) and in other reef sites subjected to
 468 low amplitude tides as well (Scoffin et al., 1985).
 469 Dating of superimposed conglomeratic beds from cross-
 470 sections at specific locations revealed mixed pictures from atoll
 471 to atoll. At Takapoto, the relevant conglomerate clasts from the
 472 southeastern *hoa* area (Fig. 4a) provided ages ranging from
 473 $3,304 \pm 12$ yr BP (SAT 102) to $1,598 \pm 12$ yr BP (SAT 112) and
 474 are systematically distributed inconsistently with respect to
 475 stratigraphy. This gives evidence that, for every individual
 476 layer, clast deposition may have occurred within a relatively
 477 long time span of about 1,500 years, within which reactivation
 478 of clasts from one phase to another seems highly likely given
 479 incomplete cementation.
 480 By contrast, in all the surveyed sites from Fakarava Atoll, the
 481 principle of stratigraphic superposition was complied with. In
 482 the southeastern rim area, in each of the three sections, the ages
 483 of clasts collected from the two-layer conglomerate platform
 484 are systematically older in the lower layer than in the upper
 485 one. At the seaward side, the lower and upper units are
 486 $5,405 \pm 28$ yr BP (FAK 28) and $3,687 \pm 11$ yr BP-old (FAK
 487 26) respectively (Fig. 7b). At the lagoonward side, clast ages
 488 from the lower unit vary between $6,250 \pm 47$ yr BP (FAK 32)
 489 and $5,449 \pm 59$ yr BP (FAK 60) while those from the upper unit
 490 range from $6,116 \pm 41$ yr BP (FAK 31) to $1,812 \pm 9$ yr BP

491 (FAK 59) respectively (Fig. 7c, d). Age differences of around
492 4,400 years between the oldest and youngest samples may
493 indicate that the implementation of the large conglomerate
494 platform in the southeastern rim at Fakarava lasted at least
495 4,000 years, starting at around 6,000 yr BP and ending less than
496 1,800 years ago. Similarly, in the 1.30-m thick, three-layer
497 conglomerate terrace capping the lagoonal reef patch E, the
498 ages of the collected clasts decrease regularly from base to top:
499 $5,017 \pm 32$ yr BP (FAK 58); $4,481 \pm 18$ yr BP; $4,149 \pm 13$ yr
500 BP (FAK 57); $4,087 \pm 43$ yr BP (FAK 55); $3,547 \pm 34$ yr BP
501 (FAK 54). Differences in age from sample to sample are about
502 150 to 1,500 years (Fig. 9c). These findings strongly suggest
503 that these conglomerate platforms have accreted over a time
504 interval not exceeding 1,500 years in length, locally with
505 depositional time recurrence of about 150 years.

506 **5 Discussion**

507 *5.1 Sources of coral clasts*

508 Works by Harmelin-Vivien and Laboute (1986), Faure and
509 Laboute (1984) and Harmelin-Vivien (1994) on some
510 northwestern Tuamotu atolls indicated that supply of coral
511 detritus to atoll-rim surfaces comes from coral communities
512 living along the upper parts of adjacent outer reef slopes. This
513 is confirmed by the taxonomic affiliation of coral clasts

514 accumulated onto reef tops, dominantly represented by
515 pocilloporid forms (Montaggioni et al., 2018).

516 A striking feature is the existence of conglomerate pavements
517 that overtop reef patches in the western and middle lagoonal
518 zones at Fakarava. In this case, the origin of coral clasts is not
519 possible to be found in the outer foreslopes. Coarse-grained
520 sediments derived from outer-reef and reef-flat zones are
521 deposited as detrital aprons along the inner lagoonal slopes.
522 Such conglomerate pavements are likely to have been built by
523 debris of coral colonies living along reef-patch slopes. Given
524 that most areas of the western rim are frequently submerged at
525 high tide, the reef rim cannot serve as a barrier to storm surges.
526 The pinnacle slopes are prone to strong waves that easily enter
527 the lagoon space, thus capable of impacting reef patches. This
528 is supported by the occurrence of about 1–2 m³, mega-blocks
529 resting on some reef patches. These blocks appear to consist of
530 individual massive *Porites* colonies, found as dominant forms
531 surrounding patches close to surface. A high consistency in
532 thickness of individual conglomerate beds is likely to reflect
533 rubble redistribution and bed reshaping by successive storm
534 events within a relatively brief time interval – a few decades.
535 However, the fact that the conglomerate platforms in the
536 lagoon at Fakarava are composed of several stacked beds
537 suggests that the successive phases of clast deposition have

538 been punctuated by gaps in clast supply, likely due to
539 decreasing storm activity at times (Fig. 12).
540 The effects of paroxysmal hazard events (storms, cyclones and
541 tsunamis) on shaping of atoll rims in the French Polynesia and
542 especially, in the Tuamotu, are poorly documented. Based on
543 radiometric dating of mega-blocks deposited on a number of
544 reef flats, Lau et al. (2016) reconstructed the history of cyclonic
545 events in the Tuamotu over the last millennium. Historical
546 records from Anaa Atoll reveal that during the 1906 cyclone,
547 the western side of the island was removed over a width of up
548 to 300 m. According to Canavesio (2014), the wave surges
549 generated during this event are likely to have reached heights
550 of up to 15–18 m. In February 1983, 4–5-m high, waves have
551 completely inundated the village at Takapoto Atoll and, on the
552 eastern side of the atoll, their impact resulted in the destruction
553 of 50 % to 100 % of the coral colonies living along the forereef
554 zone downslope to about 20 m deep (Laboute, 1985).

555 5.2 *Age of conglomerate deposition*

556 One of the critical issue to be addressed is that concerning the
557 significance of clast ages in terms of age of coral-rubble
558 deposition and stabilization. This issue has been widely debated
559 previously (Woodroffe et al., 1999, 2007; Montaggioni et al.,
560 2018). Coral elements are usually believed to have experienced
561 a short transport and rapid stabilization post-mortem. The

562 surface state and gross shape of most coral pebbles and
563 boulders indicate clearly that these have suffered repeated
564 reworking episodes prior to final stabilization. Furthermore,
565 large age discrepancies of several centuries between clasts
566 within a same bed may suggest that most clasts have undergone
567 successive cycles of reworking and redistribution since coral
568 death and before final stabilization. For instance, on the
569 southeast rim side of Takapoto Atoll, coral conglomerate clasts
570 from the same conglomerate bed provided ages of
571 $2,533 \pm 25$ yr BP (SAT 60A), $2,936 \pm 25$ yr BP (SAT 61A),
572 and $4,765 \pm 95$ yr BP (SAT 119A) respectively (**Supplementary**
573 **material**). Thus, intervals of 2,000 years at least can separate
574 extraction of individual coral colonies apparently deposited at
575 the same place by the same and last storm. By contrast, in
576 several sites, the ages of most coral clasts are clustered within
577 less than 400–1,000 years, as it is evidenced in the multiple-
578 layer conglomerates from the southeastern *hoa* system at
579 Takapoto (**Fig. 4a**) and from the two lagoonal reef patches at
580 Fakarava (**Fig. 9c**). Therefore, such age discrepancies between
581 coral clasts can be postulated as resulting from the fact that
582 coral colonies may have been retained postmortem several
583 centuries in forereef or reef-flat depocentres prior to being
584 incorporated into incipient conglomerates.

585 Even taking such effects into account, the age distributional
586 patterns of clasts into conglomerates clearly indicate that, in the

587 Tuamotu atolls under study, two-third of clasts were produced
588 within a 3,000 year time period, between 4,000 and 1,000 yr
589 BP (Fig. 10a, b). A similar pattern seems to characterize the
590 age distribution of coral clasts in conglomerate pavements at
591 the scale of the French Polynesia. Based on forty-eight U/Th-
592 dated coral specimens sampled from conglomerate units in
593 eight islands – Bora Bora, Moorea, Mataiva, Rangiroa,
594 Tikehau, Fakarava, Hao, Makemo – throughout the region,
595 Hallmann et al. (2020) demonstrated that conglomerates have
596 mainly deposited between 4,000 and 1,000 yr BP, within which
597 83 % of the dated clasts are clustered. Their maximum
598 occurrences (70% of the dated clasts) peaked between 3,000
599 and 1,000 yr BP (Fig. 10c). Finally, the integration of all the
600 ages of conglomerate clasts available for the whole French
601 Polynesian islands (145 samples) into a same frequency
602 distribution graph (Fig. 10d) reveals that up to 70 % of the
603 dated clasts have been supplied between 4,000 and 1,000 yr BP
604 and about 57 % between 3,000 and 1,000 yr BP. This clearly
605 means that in the whole French Polynesia, most of
606 conglomerate pavements have been emplaced within the same,
607 relatively short time span as suggested by Toomey et al.
608 (2013). During this interval, cyclogenesis appears to have been
609 particularly active in French Polynesia (Fig. 10d) and in other
610 tropical Pacific reef sites (Bramante et al., 2020).

611 There is similar evidence of prominent conglomerate formation
612 in a number of other Indo-Pacific reef sites, including the
613 Cocos (Keeling) Islands (Woodroffe et al., 1999), the Marshall
614 Islands (Tracey and Ladd, 1974; Buddemeier et al., 1975;
615 Kench et al., 2014b), Kiribati (Schoffield, 1977 a,b; Guinther,
616 1978), Fiji (Ash, 1987; Miyata et al., 1990) and the Cook
617 Islands (Schoffin et al., 1985; Yonekura et al., 1988; Woodroffe
618 et al., 1990c) where conglomerate clasts have provided ages
619 from about 1,200 to older than 4,000 yr BP.

620 The amount of clasts older than 4,000 yr BP in conglomerates
621 is significantly lower, rarely exceeding 20 % in all the tested
622 French Polynesian sites. The contribution of clast supply to
623 conglomerates has been very limited from 6,000 to 4,000 yr
624 BP, at a time when sea rose from its present position to about
625 +0.80 m above pmsl. One plausible explanation is that the most
626 quantities of produced detritus are likely to have just transited
627 over rim tops, prior to being stored in lagoons in the form of
628 detrital aprons, as observed at Bora Bora (Isaak et al., 2016).

629 Likewise, there are usually less than 10 % of clasts younger
630 than 1,000 yr BP in conglomerates (Fig. 10a, b, c, d). Over the
631 last millennium, coral clasts have been found to be dominantly
632 stored on atoll-rim surfaces, in the form of *motu* overlapping
633 conglomerate platforms (Montaggioni et al., 2018, 2019a).

634 5.3 Conglomerate platforms in the making

635 At Takapoto, in the northwestern rim area (Takai), within the
636 *hoa* system, there are a series of partly consolidated, chaotic
637 rubble sheets, located in front of rim islets. U/Th dates of four
638 coral samples from a 70-m long transect across these sheets are
639 provided ages younger than 1,000 yr BP: 489 ± 14 yr BP (SAT
640 21), 640 ± 14 yr BP (SAT 23), $1,685 \pm 24$ yr BP (SAT 24), and
641 586 ± 12 yr BP (SAT 26). In addition, the four additional
642 specimens collected from a nearby rubble sheet, 120 m
643 southwest of the transect, give close ages: 714, 359, 346, and
644 300 yr BP (Samuel Etienne, pers.com.) respectively. Taking
645 into account possible reworking of the oldest samples, the main
646 emplacement episode of these rubble sheets is thought to have
647 occurred between the 13th and 18th centuries. Their gross
648 morphology is quite similar to one-layer conglomerate
649 platforms. While the top surfaces of older conglomerate
650 platforms are usually regular and plate-shaped, the sheets at
651 Takai site exhibit highly uneven surfaces with numerous
652 cavities. Such a topography is likely to be due to unusually
653 powerful storm events, able to remove and deposit large coral
654 blocks. Cavities and surface irregularities are expected to be
655 clogged, smoothed and levelled by next storm-generated finer-
656 grained detritus. These deposits therefore are regarded as the
657 equivalents of conglomerate platforms in the making.

658 There is a significant development of modern rubble sheets at
659 sea level, apparently as extensive as that during the mid-late
660 Holocene, at least in a number of islands (Montaggioni and
661 Pirazzoli, 1884; Pirazzoli, 1987). This is likely due to sustained
662 cyclone activity during the past 3,000 years (Etienne and Terry,
663 2012; Toomey et al., 2013), including the last centuries
664 (Montaggioni et al., 2019a). Well-developed rubble sheets
665 mostly are accumulating in front of rim-islets, between the
666 reef-flats and the seaward sides of islets, and close to ho
667 systems where there have been still available, open surface
668 areas. Since the vast majority of detritus has been deposited
669 over islets during the last millennia, in most reef-rim areas,
670 seaward surfaces are usually occupied by shingle ridges,
671 precluding any new sediment accretion in the form of widely
672 spread, horizontal sheets.

673 *5.4 Relationships between the emplacement of conglomerate* 674 *platforms and sea level changes*

675 In the French Polynesia, as suggested by radiometric dating of
676 one hundred forty-five coral elements (Fig. 10d), deposition
677 of rubble sheets occurred principally between 3,000 and 1,000
678 yr BP through episodic storm events (“punctuated” deposition)
679 (Fig. 12). Sea level reached a maximum elevation about 0.80 m
680 above pmsl between 4,100 and 3,400 yr BP, then started to
681 drop down towards its present position (Hallmann et al., 2018,

682 2020). Given that the surfaces of conglomerate platforms are
 683 locally as high as +1.20 m to +1.80 m above pmsl
 684 (Montaggioni and Pirazzoli, 1984; Pirazzoli, 1985; Rashid et
 685 al., 2014) and the regional mean tidal range is 0.30–0.40 m,
 686 there is no ambiguous evidence: the elevation and planar
 687 surfaces of conglomerate pavements cannot be related to any
 688 supposed sea stand higher than present during the mid-late
 689 Holocene, contrary to some previous assertions (Stoddart et al.,
 690 1966).

691 The origin and conditions of conglomerate cementation in
 692 relation to sea level were discussed previously. Cements have
 693 been considered to nucleate within the modern intertidal or/and
 694 supratidal zones exposed to marine sprays (Chevalier et al.
 695 1968; Curray et al., 1970; Newell and Bloom, 1970; Chevalier
 696 and Salvat, 1976, Scoffin and McLean, 1978). The
 697 determination of lithification patterns of reef conglomerate in a
 698 number of French Polynesian Islands (Montaggioni and
 699 Pirazzoli, 1984; Pirazzoli et al., 1985) revealed that lithification
 700 took place through an early marine diagenetic sequence,
 701 vertically subdivided into two distinct subsequences: an upper,
 702 marine vadose subsequence, defined from the occurrence of
 703 grain-contact to asymmetric, gravitational cements, and a
 704 lower, phreatic subsequence, defined from isopachous fibrous
 705 to prismatic cements and/or homogeneous micrite cements
 706 partly to completely infilling intergranular voids. As

707 emphasized by McLean (2011), lithification has been probably
708 favoured by stabilization of deposits and retention of saturated
709 waters by interstitial fine-sized skeletal matrices infilling voids
710 between coarser clasts. Although its significance in terms of
711 still-sea level was recently questioned by Stoddart and Murphy
712 (2018), the physical limit between the two diagenetic
713 subsequences was assumed to delineate the position of a former
714 water marine table. This position ranges from 0.45 m to 0.95 m
715 in maximum elevation above present mean low tide level, with
716 a range of uncertainty of 0.12 m to up to 0.50 m (Montaggioni
717 and Pirazzoli, 1984), probably due in part to the upward
718 displacement of the marine phreatic zone in relation with
719 capillarity and intergranular tensional effects (Coudray and
720 Montaggioni, 1986). The diagenetic surfaces separating the two
721 subsequences may be the imprint of the relative high sea stand,
722 regionally identified from 4,100 to 3,400 yr BP (Hallmann et
723 al., 2020). At that time, sea level is inferred to have remained
724 relative stable, prior to drop at a mean rate of 0.36 mm/yr
725 (Hallmann et al., 2020). If correct, this strongly suggests that
726 sediment deposition and cementation occurred relatively
727 synchronously (Fig. 12), cementation starting as soon as
728 skeletal detritus has deposited and thus limiting reworking of
729 earlier layers by the following hazard events. This is evidenced
730 by the occurrence of multiple-layer conglomerates deposited
731 within a relatively close time interval at various atoll sites.

732 Sprays and wave surges have probably played a significant role
733 in vadose diagenesis by providing seeping waters through
734 supratidally exposed rubble layers.

735 Accretion of atoll-islands was demonstrated to have taken
736 place over the past 2,500 yr BP on Takapoto (Montaggioni et
737 al., 2019a) while conglomerate platforms were still in the
738 making. As shown by the ages of rubble sheets at present found
739 close to Takai area – north-western rim of Takapoto; (Fig.
740 4b) –, incipient conglomerate platforms were forming over the
741 last centuries. Accordingly, there has likely been interplay
742 between the development and cementation of rubble sheets and
743 the emplacement of islet nuclei. The differential responses of
744 rubble sheets and islet units to lithification are expected to have
745 been driven by the hydrologic conditions under which both
746 deposits have evolved. Conglomerates being formed have been
747 bathed in intertidal to lower supratidal zones. By contrast, rim-
748 islets and associated ridges and benches have remained in a
749 strictly sub-aerial environment, only exposed to storm wave
750 surges and rainfall. There is little evidence of early lithification
751 within rim-islet deposits. At Takapoto, detailed examination of
752 layered sedimentary units from excavated islets revealed that,
753 at some locations, small-sized cements have grown at grain
754 contacts within the lower, foraminifera-rich layers
755 (Montaggioni et al., 2018). In such cases, cementation is

756 postulated to be meteoric rather than marine in origin, due to
757 percolation of rainwaters.

758 5.5 *Conceptual model of reef conglomerate formation*

759 The conceptual model of atoll-island development previously
760 proposed for Takapoto (Montaggioni et al., 2018, 2019a) is
761 thought to be applicable to most of the neighbouring atolls in
762 the north-western Tuamotu and as such, to Takaroa and
763 Fakarava. Specifically focused on the conditions of
764 emplacement of conglomerate pavements, the model is as
765 follows (Fig. 13). While sea level exceeded its present position
766 by about 6,000 BP and continued to rise to about 0.8 m above
767 pmsl until 4,000 yr BP (Hallmann et al., 2018, 2020), the tops
768 of reef rims in the northwestern Tuamotu were still submerged
769 and accreting upwards to catch up with sea level. Rim surfaces
770 are likely have approximated sea level by around 5,500 yr BP
771 (Hallmann et al., 2020). At that time, storm-generated wave
772 surges have been able to supply reef-rim surfaces with coral
773 clasts. However, based on the relative low amount of coral
774 clasts older than 4,000 yr BP, most of those has possibly been
775 moved across atoll-rims and deposited along the inner lagoonal
776 slopes as detrital aprons. According to the average age of
777 conglomerate clasts, initial rubble sheets are interpreted to have
778 mainly accreted within a 2,000-year-long interval, between
779 3,000 and 1,000 yr BP at the time when sea level dropped

780 regularly to present sea level (Hallmann et al., 2020). However,
781 it is noteworthy that as the sea level got lower, the platforms
782 still got higher through successive additions of beds.
783 Cementation is thought to have operated relatively coevally
784 with clast deposition, thereby allowing initial rubble sheets to
785 be stabilized and consolidated in the form of stacked, multiple-
786 layer conglomerate pavements.

787 *5.6 Evaluating the role of conglomerate platforms as*
788 *protectors of low-lying reef islands in the future.*

789 There is an ongoing concern regarding the possibility of low-
790 island submergence and disappearance in the future due to sea-
791 level rise (Yamano et al., 200; Hubbard et al. 2014; McLean
792 and Kench, 2015; Quataert et al., 2015; van Woesik et al.,
793 2015; Vitousek et al., 2016; Kuffner, 2018; Storlazzi et al.,
794 2015, 2018; Kulp and Strauss, 2019), especially when taking
795 into account the extreme projections inferred from probabilistic
796 process-based models as those by Kopp et al (2017) and Le
797 Bars et al. (2017). It is predicted that the rise in sea level would
798 reach heights of 2.00 m or more above present by AD 2100.
799 Median scenarios postulate a sea level approximating 1 m
800 above pmsl at that time (IPCC, 2019) particularly in French
801 Polynesia (Botella, 2015). According to such scenarios, thicker
802 conglomerate pavements would be moved from supratidal to
803 intertidal zones or, in other words, passing from marine vadose

804 to phreatic, diagenetic environments. In conglomerates and
805 beach-rocks as well, marine cementation is known to operate
806 rapidly under phreatic conditions, resulting in the precipitation
807 of structureless micrite matrices and isopachous fringes of
808 fibrous and prismatic cements and a significant loss of porosity
809 (Newell and Bloom, 1970; Scoffin and Stoddart, 1983;
810 Coudray and Montaggioni, 1986; Montaggioni and Pirazzoli,
811 1984). Conglomerates would become more firmly consolidated
812 and serve as wave breakers in association to or in place of
813 adjacent reef crests. The water table as following the rising
814 course of sea level would flood progressively through the lower
815 parts of reef-rim islets. In the event of their relative stability
816 over several decades, the relevant deposits would be probably
817 affected by marine to meteoric cementation as previously
818 observed at the base of some excavated islet sections on
819 Takapoto (Montaggioni et al., 2018). Reinforcing of islet
820 basements would help better withstanding disturbances related
821 to sea-level rise and expected increasing storminess.
822 Furthermore, in healthy reef areas, sea-level rise would
823 promote coral growth, reef structural complexity and vertical
824 reef-flat accretion. The maintenance of structural complexity is
825 regarded as critical to ensure protection of tropical shorelines
826 (Harris et al., 2018). Such a scenario has been reported from
827 Moruroa Atoll, southeastern end of Tuamotu (Faure *in* Bablet
828 et al., 1995; Levrel, 2009). On this atoll, coral cover rates and

829 species abundance have been estimated from about 1-m-
830 deepened, healthy reef-flats as a consequence of collapsing
831 caused by underground nuclear tests. Surveys conducted in
832 1992 and 2009 revealed clearly that reef-flat deepening has
833 favored settlement of branching, fast-growing coral forms
834 (*Pocillopora*, *Acropora*). Cover rates have increased from
835 4.1 % to 11.3 % of the total substrate surfaces, species richness
836 from 7 to 23, mean colony diameter from 12.4 cm to 35.6 cm.
837 Vertical growth predominates over lateral extension as it aims
838 at catching up with sea level. If applicable to the coming
839 decades, although the main coral source is known to be the
840 upper forereef zone (Harmelin-Vivien and Laboute, 1986), this
841 model suggests that increasing volumes of coral fragments
842 would be available from closer sources for further rubble-sheet
843 and islet accretion or for compensating for islet erosion.
844 Moreover, reef growth-modes on other French Polynesian
845 islands will differ, depending on local environmental
846 constraints. In the case of keeping-up mode, as experienced by
847 the Tahitian barrier-reef crest during the Holocene
848 (Montaggioni et al., 1997), outer reef crests may be protective
849 of islets against storm surges. In the case of catching-up mode,
850 wave surges will break directly on shores due to submergence
851 of reef-crest lines. In relation to this case, conglomerate
852 platforms will become the first and only line of defence.

853 As emphasized by Duvat (2018), different atoll islands have
854 responded differentially to sea level rise over the last decades,
855 from size increase, maintenance to reduction. According to
856 exposure, islands have suffered slight to severe reshaping. In
857 the future, in relation to up to 1-m rise in sea level, island
858 reworking could be amplified to partial destruction.
859 Consolidation of conglomerates, partial lithification of loose
860 islets and increasing coral-clast production could be pivotal
861 processes to the maintenance of low-lying reef islands in the
862 long term.

863 **6 Conclusions**

864 Field examination of cemented conglomerate platforms
865 indicate that in French Polynesia and more specifically in the
866 northwestern Tuamotu, these platforms are widely spread
867 structures, extending over reef-rim surfaces locally from the
868 seaward shoreline to the borders of lagoons. These serve as
869 foundations for reef-rim islands. Initially deposited as rubble
870 sheets, composed of one-single to several superimposed layers,
871 the conglomerates are about +0.50 m to up to +1.50 m in
872 elevation above pmsl. This highlights the critical role of storm-
873 generated wave surges in the emplacement of rubble sheets and
874 atoll-island shaping.

875 Radiometric dating of individual coral clasts trapped into
876 conglomerates indicate that deposition took place mainly

877 within an about 2,000 year-time window from 3,400 to 1,300 yr
878 BP, during a sea-level drop of about 0.80 m in amplitude.
879 Between 6,000 and 4,000 yr BP, the most amount of detrital
880 production is likely to have been prominently accumulated in
881 lagoons, resulting in the formation of sediment aprons.
882 The timing and mode of clast deposition appear to have varied
883 significantly from site to site. In some cases, individual
884 conglomerate layers have been deposited within a relatively
885 short-time range (500 to < 1,000 years) and experienced limited
886 clast reworking. In other occurrences, deposition of layers may
887 have needed more time (about 1,500 years) and has presumably
888 been followed by intense disturbance.
889 Despite the potential effects of cyclic clast reworking on
890 deposition, final stabilization and lithification of original rubble
891 sheets are expected to have occurred coevally, as evidenced by
892 the stacking of several, distinct and firmly lithified layers.
893 Some layers may have deposited during a discrete hazard
894 event. These processes have been demonstrated to occur within
895 marine, phreatic and vadose environments during the course of
896 falling sea level over the mid-late Holocene. Higher sea level,
897 periodic spraying and flooding of conglomerate outcrops by
898 waves are likely to have favored early cementation.
899 Dating of rubble sheets at specific atoll-rim locations also
900 indicates that incipient conglomerate pavements have started to
901 form a few centuries ago while sea level was close to present.

902 The most striking feature is the interplay between the formation
903 of cemented conglomerate platforms and the development of
904 reef-rim islands. These two depositional events have operated
905 concomitantly over a 1,500-year long period, between about
906 2,500 and 1,000 yr BP, but under different hydrologic
907 conditions. Conglomerate formation has occurred within the
908 intertidal to supratidal zone, while islets have accreted
909 subaerially. This may explain differential responses of each
910 deposit type to lithification. The interplaying process seems to
911 have been interrupted in response to the sea-level retreat over
912 the last 1,000 years. The continued sea level rise in the future
913 could be accompanied by partial re-flooding of both
914 conglomerate beds in the making and the lower sections of
915 atoll-rim islands, thus resulting in the resumption of the
916 interplaying process.

917 Although distributed non-uniformly on atoll rims,
918 conglomerate platforms are expected to play a protective role
919 for unconsolidated atoll-rim islands against potential erosion
920 due to sea-level rise and increasing storminess. Protection
921 would be reinforced as the ongoing sea-level rise promotes not
922 only further conglomerate consolidation, but also incipient islet
923 cementation and sustained coral reef growth. Conglomerates
924 are assumed to be key structures for the maintenance of atoll
925 islands in the future. Accordingly, predicting changes in the
926 morphological evolution of low-lying reef islands requires a

927 detailed knowledge of morphology and distribution of
928 conglomerate platforms as a prerequisite.

929 **Acknowledgements**

930 This work was supported by the French National 791 Research
931 Agency (CNRS) under the STORISK research project (N_
932 ANR-15-CE03-0003). Field work has benefited from logistical
933 support by the Research Station of the Office of Marine
934 Resources in Takapoto and Takaroa during early March 2018
935 and by Gaby Maiti Haumani, Hugo Dayan and Pascale
936 Braconnot in Fakarava during mid-March 2019. Many thanks
937 to the two anonymous reviewers whose comments have
938 significantly helped improving an early version of the
939 manuscript.

940 **Research data**

941 All research data are available following this link:
942 <https://amubox.univ-amu.fr/s/jbMPaKfPM9CD9BS>

943 **References**

944 [Andréfoüet, S., Ardhuin, F., Queffelec, P., Le Gendre, R.,](#)
945 [2012. Island shadow effect and the wave climate of the](#)
946 [Western Tuamotu Archipelago \(French Polynesia\) inferred](#)
947 [from altimetry and numerical model data. Marine](#)
948 [Pollution Bulletin 65, 415–424.](#)

949 Andréfouët, S., Genthon, P., Pelletier, B., Le Gendre, R., Friot,
 950 C., Smith, R., Liao, V., 2020. The lagoon geomorphology
 951 of pearl farming atolls in the Central Pacific Ocean
 952 revisited using detailed bathymetric data. *Marine*
 953 *Pollution Bulletin* 160, 111580.

954 Bablet J.P., Gout B. et Goutière G., 1995. Les atolls de Mururoa
 955 et de Fangataufa, III, Le milieu vivant et son évolution.
 956 Commissariat à l'Energie Atomique. Direction des
 957 Applications Militaires/ Direction des essais, p. 1–308.

958 Becker, M., Meyssignac, B., Letetrel, C., Llovel, W., Cazenave,
 959 A., Delcroix, T., 2012. Sea level variations at tropical
 960 Pacific islands since 1950. *Global and Planetary Change*,
 961 80–81, 85–98.

962 Beetham, E., Kench, P.S., Popinet, S., 2017. Future reef growth
 963 can mitigate physical impacts of sea-level rise on atoll
 964 islands. *Earth's Future* 5, 102–114.

965 Bhatia, K., Vecchi, G., Murakami, H., Underwood, S., Kossin,
 966 J., 2018. Projected response of tropical cyclone intensity
 967 and intensification in a global climate model. *Journal of*
 968 *Climate* 31, 8281–8303. [https://doi.org/10.1175/JCLI-D-](https://doi.org/10.1175/JCLI-D-17-0898.1)
 969 [17-0898.1](https://doi.org/10.1175/JCLI-D-17-0898.1)

970 Bongers, Th., Wyrski, K., 1987. Sea level at Tahiti – a minimum
 971 of variability. *Journal of Physical Oceanography* 17, 164–
 972 168.

973 Botella, A., 2015. Past and future sea level changes in French
 974 Polynesia. University of Ottawa, Canada, MSc.Thesis,
 975 94 p.

976 Bouchon, C., 1983. Les peuplements de scléractiniaires de
 977 l'atoll de Takapoto (Polynésie Française). *Journal de la*
 978 *Société des Océanistes* 77, 35–42.

979 Bramante, J.F., Ashton, A.D., Storlazzi, C.D., Cheriton, O.M.,
 980 Donnelly, J.P. 2020a. Sea level rise will drive divergent
 981 sediment transport patterns on fore reefs and reef flats,
 982 potentially causing erosion on atoll islands. *Journal of*
 983 *Geophysical Research: Earth Surface*, 125,
 984 e2019JF005446. [https://doi.org/ 10.1029/2019JF005446](https://doi.org/10.1029/2019JF005446)

985 Bramante, J.F., Ford, M.R., Kench, P.S., Ashton, A.D., Toomey,
 986 M.R., Sullivan, R.M., Karnauskas, K.B., Ummenhofer,
 987 C.C., Donnelly, J.P., 2020b. Increase typhoon activity in
 988 the Pacific deep tropics driven by Little Ice Age
 989 circulation changes. *Nature Geoscience* 13, 806–811; doi:
 990 10.1038/s41561-020-00656-2

991 Buddemeier, R.W., Smith, S.V., Kinzie, R.A., 1975. Holocene
 992 windward reef-flat history, Enewetak Atoll. *Geological*
 993 *Society of America Bulletin* 86, 1581–1584.


994 Canavesio, R., 2014. Estimer les houles cycloniques à partir
 995 d'observations météorologiques limitées exemple de la
 996 submersion d'Anaa en 1906 aux Tuamotu (Polynésie
 997 Française). *Vertigo* 14. doi.org/10.4000/vertigo.15375.

998 Cheal, A.J., MacNeil, M.A., Emslie, M.J., Sweatman, H., 2017.
 999 The threat to coral reefs from more intense cyclones under
 1000 climate change. *Global Change Biology* 23, 1511–1524.

1001 Cheng, H., Edwards, R.L., Hoffa, J., Gallup, C.D., Richards,
 1002 D.A., Asmerom, Y., 2000. The half- lives of uranium-234
 1003 and thorium-230. *Chemical Geology* 169, 17–33.

1004 Cheng, H., Lawrence Edwards, R., Shen, C.-C., Polyak, V.J.,
1005 Asmerom, Y., Woodhead, J.D., Hellstrom, J., Wang, Y.,
1006 Kong, X., Spötl, C., Wang, X., Calvin Alexander, E.,
1007 2013. Improvements in ^{230}Th dating, ^{230}Th and ^{234}U half-
1008 life values, and U/Th isotopic measurements by multi-
1009 collector inductively coupled plasma mass spectrometry.
1010 Earth and Planetary Science Letters 371–372, 82–91.

1011 Chevalier, J.-P., Denizot, M., Mougín, J.L., Plessis, Y., Salvat,
1012 B., 1968. Étude géomorphologique et bionomique de
1013 l'atoll de Mururoa (Tuamotu). Cahiers du Pacifique 12, 1–
1014 144.

1015 Chevalier, J.P., Denizot, M., Ricard, M., Salvat, B., Sournia, A.,
1016 Vasseur, P., 1979. Géomorphologie de l'atoll de Takapoto.
1017 Journal de la Société des Océanistes 35, 9–18. 

1018 Clark, P.U., Shakun, J.D., Marcott, S.A., Mix, A.C., Eby, M.,
1019 Kulp, S., Levermann, A., Milne, G.A., Pfister, P.L.,
1020 Santer, B.D., Schrag, D.P., 2016. Consequences of twenty-
1021 first-century policy for multi-millennial climate and sea-
1022 level change. Nature Climate Change 6, 360–369.

1023 Clouard, V., Bonneville, A., 2003. Submarine landslides in
1024 Society and Austral islands, French Polynesia: evolution
1025 with the age of edifices. In: Locat, J., Mienert, J.,
1026 Boisvert, L. (eds), Submarine mass movements and their
1027 consequences, Springer, p. 335–341.

1028 Clouard, V., Bonneville, A., 2004. Submarine landslides in
1029 French Polynesia. In: Hekinian, R., Cheminée, J.-L.,
1030 Stoffers, P. (eds), Oceanic Hotspots, Springer, p. 209–
1031 238.

1032 Coudray J., Montaggioni L., 1986. The diagenetic products of
1033 marine carbonates as sea-level indicators. In: van de
1034 Plassche O. (ed) Sea-Level Research. Springer, Dordrecht.
1035 https://doi.org/10.1007/978-94-009-4215-8_11

1036 Curray, J.R., Shepard, F.P., Veeh, H.H., 1970. Late Quaternary
1037 sea level studies in Micronesia. CARMARSEL Expedition.
1038 Geological Society of America Bulletin 81, 1865–1880.

1039 Delesalle, B., 1985. Mataiva atoll. Proceedings of the 5th
1040 International Coral Reef Congress 1, 269–322.

1041 Duvat, V.K.E., 2018. A global assessment of atoll island
1042 planform changes over the past decades. WIREs Climate
1043 Change 2018;e557. DOI: 10.1002/wcc.557

1044 Duvat, V.K.E., Pillet, V., 2017. Shoreline changes in reef
1045 islands of the Central Pacific: Takapoto Atoll, Northern
1046 Tuamotu, French Polynesia. Geomorphology 282, 96–118.

1047 Duvat, V.K.E., Pillet, V., Volto, N., Terorotua, H., Laurent, V.,
1048 2020. Contribution of moderate climate events to atoll
1049 island building (Fakarava Atoll, French Polynesia).
1050 Geomorphology 354, 107057.

1051 East, H.K., Perry, C.T., Kench, P.S., Liang, Y., Gulliver, P.,
1052 2018. Coral reef island initiation and development under
1053 higher than present sea levels. Geophysical Research
1054 Letters 45, 11,265-11,274.

1055 East, H.K., Perry, C.T., Beetham, E.P., Kench, P.S., Liang, Y.,
1056 2020. Modelling reef hydrodynamics and sediment
1057 mobility under sea level rise in atoll reef systems. Global
1058 and Planetary Change 192, 103196.

1059 Emanuel, K., 2007. Environmental factors affecting tropical
1060 cyclone power dissipation. *Journal of Climate* 20, 5497–
1061 5509.

1062 Etienne, S., 2012. Marine inundation hazards in French 896
1063 Polynesia: geomorphic im- pacts of Tropical Cyclone Oli
1064 in February 2010. In: Terry, J.P., Goff, J. (Eds.), *Natural*
1065 *Hazards in the Asia-Pacific Region: Recent Advances and*
1066 *Emerging Concepts*. Geological Society of London,
1067 Special Publication, 361, 21–39.

1068 Etienne, S., Terry, J.P., 2012. Coral boulders, gravel tongues
1069 and sand sheets: Features of coastal accretion and
1070 sediment nourishment by Cyclone Tomas (March 2010) on
1071 Taveuni Island, Fiji. *Geomorphology* 175–176, 54–65.

1072 Faure, G., Laboute, P., 1984. Formations récifales 1: Définitions
1073 des unités récifales et distribution des principaux
1074 peuplements de scléactiniaires. In: *L’atoll de Tikehau*
1075 *(Archipel des Tuamotu, Polynésie française), Premiers*
1076 *Résultats. Notes et Documents Océanographiques* 22,
1077 ORSTOM, 108–136.

1078 Fietzke, J., Liebetrau, V., Eisenhauer, A., Dullo, C.W., 2005.
1079 Determination of uranium iso- tope ratios by multi-static
1080 MIC-ICP-MS: method and implementation for precise U-
1081 and Th-series isotope measurements. *Journal of Analytical*
1082 *Atomic Spectrometry* 20, 395–401.

1083 Gabriél, C., Salvat, B., 1985. General features of French
1084 Polynesian Islands and their coral reefs. *Proceedings of*
1085 *the 5th International Coral Reef Congress* 1, 1–16.

1086 Guinther, E.B., 1978. Observations on terrestrial surface and
1087 subsurface water as related to island morphology at
1088 Canton atoll. *Atoll Research Bulletin* 221, 171–183.


1089 Hallmann, N., Camoin, G., Eisenhauer, A., Botella, A., Milne,
1090 G.A., Vella, C., Samankassou, E., Pothin, V., Dussouillez,
1091 P., Fleury, J., Fietzke, J., 2018. Ice volume and climate
1092 changes from a 6000 year sea-level record in French
1093 Polynesia. *Nature Communications* 9. [https://doi.](https://doi.org/10.1038/s41467-017-02695-7)
1094 [org/10.1038/s41467-017-02695-7](https://doi.org/10.1038/s41467-017-02695-7).

1095 Hallmann, N., Camoin, G., Eisenhauer, A., Samankassou, Vella,
1096 C., Botella, A., Milne, G.A., Pothin, V., Dussouillez, P.,
1097 Fleury, G., Fietzke, J., Goepfert, G., 2020. Reef response
1098 to sea level and environmental changes in the Central
1099 South Pacific over the past 6000 years. *Global and*
1100 *Planetary Change* 195, 103357.

1101 Harmelin-Vivien, M.L., 1994. The effects of storms and
1102 cyclones on coral reefs: a review. *Journal of Coastal*
1103 *Research, Special Issue, Coastal Hazards*, 12, 211–231.

1104 Harmelin-Vivien, M.L., Laboute, P., 1986. Catastrophic impact
1105 of hurricanes on atoll outer reef slopes in the Tuamotu
1106 (French Polynesia). *Coral Reefs* 5, 55–62.

1107 Harris, D.L., Rovere, A., Casella, E., Power, H., Canavesio, R.,
1108 Collin, A., Pomeroy, A., Webster, J. M., Parravicini, V.,
1109 2018. Coral reef structural complexity provides important
1110 coastal protection from waves under rising sea levels.
1111 *Science Advances* 4:eaao4350

1112 Hay, C.C., Morrow, E., Kopp, R.E., Mitrovica, J.X., 2015.
 1113 Probabilistic reanalysis of twentieth-century sea-level
 1114 rise. *Nature* 517 (7535), 481–484. 

1115 Heaton, T.J., Köhler, P., Butzin, M., Bard, E., Reimer, R.W.,
 1116 Austin, W.E.N., Bronk Ramsey, C., Hughen, K.A.,
 1117 Kromer, B., Reimer, P.J., Adkins, J., Burke, A., Cook,
 1118 M.S., Olsen, J., Skinner, L.C., 2020. Marine20-the marine
 1119 radiocarbon age calibration curve (0-55,000 cal BP).
 1120 *Radiocarbon* 62. doi: 10.1017/RDC.2020.68.

1121 Holland, G. J., Done, J. M., Douglas, R., Saville, G. R., Ge, M.,
 1122 2019. Global tropical cyclone damage potential. In J.
 1123 Collins, K. Walsh (Eds.), *Hurricane risk*, Springer, pp.
 1124 23–42.


1125 *Radiocarbon* 62. doi: 10.1017/RDC.2020.68.

1126 Holland, G. J., Done, J. M., Douglas, R., Saville, G. R., Ge, M.,
 1127 2019. Global tropical cyclone damage potential. In J.
 1128 Collins, K. Walsh (Eds.), *Hurricane risk*, Springer, pp.
 1129 23–42.

1130 Horton, B.P., Khan, N.S., Lee, J.S.H., Shaw, T.A., Garner, A.J.,
 1131 Kemp, A.C., Engelhart, S.E., Rahmstorf, S., 2020.
 1132 Estimating global mean sea-level rise and its uncertainties
 1133 by 2100 and 2300 from an expert survey. *Climate and*
 1134 *Atmospheric Science* 3, 18.

1135 Hubbard, D., Gischler, E., Davies, P., Montaggioni, L.F.,
 1136 Camoin, G., Dullo, C.W., Storlazzi, C., Field, M.,
 1137 Fletcher, C., Grossman, E., Sheppard, C., Lescinsky, H.,
 1138 Fenner, D., McManus, J., Scheffers, S., 2014. Island
 1139 outlook: warm and swampy. *Science* 345 (6203).

1140 IPCC, 2019, Special Report on the Ocean and Cryosphere in a
 1141 Changing Climate (Pörtner H.O. Roberts, D.C.,
 1142 MassonDelmotte, V., Zhai, P., Tignor, M., Poloczanska,
 1143 E., Mintenbeck, K., .Alegría, A., Nicolai, M., Okem, A.,
 1144 Petzold, J., Rama, B., Weyer, N.M. (eds.), 35 pp.

1145 Jaffey, A.H., Flynn, K.F., Glendenin, L.E., Bentley, W.C.,
 1146 Essling, A.M., 1971. Precision measurements of half-lives
 1147 and specific activities of ^{235}U and ^{238}U . Physical Review
 1148 C4, 1889–1906. 

1149 Kench, P.S., Owen, S.D., Ford, M.R., 2014a. Evidence for coral
 1150 island formation during rising sea level in the central
 1151 Pacific Ocean. Geophysical Research Letters 41, 820–827.

1152 Kench, P.S., Chan, J., Owen, S.D., McLean, R.F., 2014b. The
 1153 geomorphology, development and temporal dynamics of
 1154 Tepuka Island, Funafuti atoll, Tuvalu. Geomorphology
 1155 222, 46–58.

1156 Kench, P.S., Thompson, D., Ford, M.R., Ogawa, H., McLean,
 1157 R.F., 2015. Coral reef islands defy sea-level rise over the
 1158 past century: records from a central Pacific atoll. Geology
 1159 43, 515–518.

1160 Knutson, T. R., McBride, J.L., Chan, J., Emanuel, K., Holland,
 1161 G., Landsea, C., Held, I., Kossin, J.P., Srivastava, A.K.,
 1162 Sugi, M., 2010. Tropical cyclones and climate change.
 1163 Nature Geoscience 3, 157–163.

1164 Kopp, R.E., Horton, R.M., Little, C.M., Mitrovica, J.X.,
 1165 Oppenheimer, M., Rasmussen, D.J., Strauss, B.H.,
 1166 Tebaldi, C., 2014. Probabilistic 21st and 22 nd century

1167 sea-level projections at a global network of tide-gauge
1168 sites. *Earth's Future* 2, 383–406.

1169 Kopp, R. E., DeConto, R. M., Bader, D. A., Hay, C. C., Horton,
1170 R. M., Kulp, S., Oppenheimer, M., Pollard, D. and
1171 Strauss, B. H., 2017. Evolving Understanding of Antarctic
1172 Ice-Sheet Physics and Ambiguity in Probabilistic Sea-
1173 Level Projections. *Earth's Future* 5, 1217–1233.

1174 Kossin, J.P., Knapp, K.R., Olander, T. L., Velden, Ch. S., 2020.
1175 Global increase in major tropical cyclone exceedance
1176 probability over the past four decades. *PNAS* 117, 11975–
1177 11980.

1178 Kuffner, I.B., 2018. Sea level could overwhelm coral reefs.
1179 *Nature* 558, 378–379.

1180 Kühlmann, H.H., Chevalier, J.-P., 1986. Les coraux
1181 (Scléactiniaires et hydrocoralliaires) de l'atoll de
1182 Takapoto, îles Tuamotu: aspects écologiques. *Marine*
1183 *Ecology Progress Series* 7, 75–104.

1184 Kulp, S.A., Strauss, B.H., 2019. Double elevation data triple
1185 estimates of global vulnerability to sea-level rise and
1186 coastal flooding. *Nature Communications* 10:4844 |
1187 <https://doi.org/10.1038/s41467-019-12808-z>

1188 Laboute, P., 1985. Evaluation of damage done by the cyclones
1189 of 1982-1983 to the outer slopes of the Tikehau and
1190 Takapoto Atolls (Tuamotu Archipelago). *Proceedings of*
1191 *the 5th International Coral Reef Congress, Tahiti* 3, 323–
1192 329.

1193 Larrue, S., Chiron, Th., 2010. Les îles de Polynésie Française
1194 face à l'aléa cyclonique. *Vertigo* 10.
1195 doi.org/10.4000/vertigo.10558.

1196 Lau, A.Y.A., Terry, J.P., Switzer, A.D., Lee, Y., Etienne, S.,
1197 2016. Understanding the history of extreme wave events
1198 in the Tuamotu Archipelago of French Polynesia from
1199 large carbonate boulders on Makemo Atoll, with
1200 implications for future threats in the central South Pacific.
1201 *Marine Geology* 380, 174–190.

1202 Le Bars, D., Drijfhout, S. and Vries, H., 2017. A high-end sea
1203 level rise probabilistic projection including rapid
1204 Antarctic ice sheet mass loss. *Environmental Research*
1205 *Letters* 12, 044013.

1206 Levrel, A., 2010. Colonisation corallienne d'une zone
1207 submergée : exemple de Mururoa. RA 177, CRIOBE, USR
1208 3278 EPHE-CNRS-UPVD, Moorea, Polynesia, and
1209 Perpignan, p.1–72.

1210 Lin, I.I., Goni, G.J., Knaff, J.A., Forbes, C., Ali, M.M., 2013.
1211 Ocean heat content for tropical cyclone intensity
1212 forecasting and its impact on storm surge. *Natural*
1213 *Hazards*, 66, 1481-1500.

1214 Liu, M., Vecchi, G.A., Smith, J., Knutson, T., 2019. Storm
1215 intensification and increased water vapor explain the
1216 super-Clausius-Clapeyron increase of tropical cyclone
1217 rainfall under global warming. *NPJ Climate and*
1218 *Atmospheric Science*. doi:10.1038/s41612-019-0095-3.

- 1219 Masselink, G., Beetham, E., Kench, P., 2020. Coral islands can
1220 accrete vertically in response to sea level rise. *Science*
1221 *Advances*, 6: eaay3656
- 1222 McLean, R., 2011a. Atoll islands (motu). In: Hopley, D. (ed)
1223 *Encyclopedia of Modern Coral Reefs. Encyclopedia of*
1224 *Earth Sciences Series. Springer, Dordrecht, pp.47–51.*
1225 doi.org/10.1007/978-90-481-2639-2_201
- 1226 McLean, R., 2011b. Platforms (cemented). In: Hopley, D. (ed)
1227 *Encyclopedia of Modern Coral Reefs. Encyclopedia of*
1228 *Earth Sciences Series. Springer, Dordrecht, pp.812.*
1229 https://doi.org/10.1007/978-90-481-2639-2_201
- 1230 McLean, R.F., Hosking, P.L., 1991. Geomorphology of reef
1231 islands and atoll motu in Tuvalu. *South Pacific Journal of*
1232 *Natural Science* 11, 167–189.
- 1233 McLean, R.F., Kench, P., 2015. Destruction or persistence of
1234 coral atoll islands in the face of 20th and 21th century
1235 sea-level rise? *WIREs Climate Change* 6, 445–463.
- 1236 Miyata, T., Maeda, Y., Matsumoto, E., Matsushima, Y., Rodda,
1237 P., Sugimura, A., Kayanne, H., 1990. Evidence for a
1238 Holocene high sea-level stand, Vanua Levu, Fiji.
1239 *Quaternary Research* 33, 352–359.
- 1240 Montaggioni, L.F., 2011. Conglomerates. In: Hopley, D. (ed)
1241 *Encyclopedia of Modern Coral Reefs. Encyclopedia of*
1242 *Earth Sciences Series. Springer, Dordrecht, pp.229–230.*
1243 doi.org/10.1007/978-90-481-2639-2_201
- 1244 Montaggioni, L.F., Pirazzoli, P.A., 1984. The significance of
1245 exposed coral conglomerates from French Polynesia

1246 (Pacific Ocean) as indications of recent sea-level changes.
1247 Coral Reefs 3, 29–42.

1248 Montaggioni, L.F., Cabioch, G., Camoin, G.F., Bard, E.,
1249 Ribaud-Laurenti, A., Faure, G., 1997. Continuous record
1250 of reef growth over the past 14 kyr on the mid-Pacific
1251 island of Tahiti. *Geology* 25, 555–558.

1252 Montaggioni, L.F., Salvat, B., Aubanel, A., Eisenhauer, A.,
1253 Martin-Garin, B., 2018. The mode and timing of windward
1254 reef-island accretion in relation with Holocene sea-level
1255 change: a case study from Takapoto Atoll, French
1256 Polynesia. *Geomorphology* 318, 320–335.

1257 Montaggioni, L.F., Salvat, B., Aubanel, A., Pons-Branch, E.,
1258 Martin-Garin, B., Dapoigny, A., Goeldner-Gianella,
1259 2019a. New insights into the Holocene development
1260 history of a Pacific low-lying coral island: Takapoto
1261 Atoll, french Polynesia. *Quaternary Science Reviews* 223,
1262 105947.

1263 Montaggioni, L.F., Collin, A., James, D., Bernard, S., Martin-
1264 Garin, B., Siu, G., Taiarui, M., Chancerelle, Y., 2019b.
1265 Morphology of fore-reef slopes and terraces, Takapoto
1266 Atoll (Tuamotu Atoll, French Polynesia, central Pacific):
1267 the tectonic, sea-level and coral-growth control. *Marine*
1268 *Geology* 417, 106027.

1269 Newell, N.D., Bloom, A.L., 1970. The reef flat and « two meter
1270 eustatic terrace » of some Pacific atolls. *Geological*
1271 *Society of America Bulletin* 81, 1881–1894.

1272 Pagès, J., Andréfouët, S., Delesalle, B., Prasil, V., 2001.
1273 Hydrology and trophic state in Takapoto Atoll lagoon:

- 1274 comparison with other Tuamotu lagoons. *Aquatic Living*
1275 *Resources* 14, 183–193.
- 1276 Pala, C., 2014. Warming may not swamp islands. *Science* 345,
1277 496–497.
- 1278 Petchey, F., Anderson, A., Hogg, A.G., Zondervan, A., 2008.
1279 The marine reservoir effect in the Southern Ocean: An
1280 evaluation of extant and new Delta-R values and their
1281 application to archaeological chronologies. *Journal of the*
1282 *Royal Society of New Zealand* 38:4, 243–262.
- 1283 Pirazzoli, P.A., 1987. A reconnaissance and geomorphological
1284 survey of Temoe Atoll, Gambier Islands (South Pacific).
1285 *Journal of Coastal Research* 3, 307–323.
- 1286 Pirazzoli, P.A., 1985. Leeward Islands: Maupiti, Tupai, Bora
1287 Bora, Huahine, Society Archipelago. *Proceedings of the*
1288 *5th International Coral Reef Congress, Tahiti* 1, 17–72.
- 1289 Pirazzoli, P.A., Montaggioni, L.F., 1986. Late Holocene
1290 changes in the northwest Tuamotu Islands, French
1291 Polynesia. *Quaternary Research* 25, 350–368.
- 1292 Pirazzoli, P.A., Montaggioni, L., 1988a. The 7000 year sea-level
1293 curve in French Polynesia: geodynamic implications for
1294 mid- plate volcanic islands. *Proceedings of the 6th*
1295 *International Coral Reef Symposium, Townsville* 3, 467–
1296 472.
- 1297 Pirazzoli, P.A., Montaggioni, L.F., 1988b. Holocene sea-level
1298 changes in French Polynesia. *Palaeogeography,*
1299 *Palaeoclimatology, Palaeoecology* 68, 153–175.
- 1300 Pirazzoli, P.A., Montaggioni, L.F., Delibrias, G., Faure, G.,
1301 Salvat, B., 1985. Late Holocene sea-level changes in the

1302 Society Islands and the north-west Tuamotu atolls.
1303 Proceedings of the 5th International Coral Reef Congress,
1304 Tahiti, 3, 131–136.


1305 Pirazzoli, P.A., Delibrias, G., Montaggioni, L.F., Saliège, F.,
1306 Vergnaud-Grazzini, C., 1987a. Vitesse de croissance
1307 latérale des platiers et évolution morphologique récente de
1308 l’atoll de Reao, îles Tuamotu, Polynésie Française.
1309 Annales de l’Institut Océanographique 63, 57–68.

1310 Pirazzoli, P.A., Montaggioni, L.F., Vergnaud-Grazzini, C.,
1311 Saliège, J.F., 1987b. Late Holocene sea levels and coral
1312 reef development in Vahitahi Atoll, eastern Tuamotu
1313 Islands, Pacific Ocean. Marine Geology 76, 105–116.

1314 Pirazzoli, P.A., Montaggioni, L.F., Salvat, B., Faure, G., 1988.
1315 Late Holocene sea level indicators from twelve atolls in
1316 the central and eastern Tuamotus (Pacific Ocean). Coral
1317 Reefs 7, 57–68.

1318 Pons-Branchu, E., Douville, E., Dumont, E., Branchu, P., Thil,
1319 F., Frank, N., Bordier, L., Borst, W., 2014. Cross-dating
1320 (U/Th and lamina counting) of modern carbonate deposits
1321 in underground Paris, France. A new archive for urban
1322 history re- constructions: case study of anthropic Rare
1323 Earth and Yttrium release. Quaternary Geochronology 24,
1324 44–53.

1325 Puotinen, M., Drost, E., Lowe, R., Depczynski, M., Radford, B.,
1326 Heyward, A., Gilmour, J., 2020. Towards modelling the
1327 future risk of cyclone wave damage to the world’s coral
1328 reefs. Global Change Biology. doi: 10.1111/gcb.15136

- 1329 Quataert, E., Storlazzi, C., van Rooijen, A., Cheriton, O., van
1330 Dongeren, A., 2015. The influence of coral reefs and
1331 climate change on wave-driven flooding of tropical
1332 coastlines. *Journal of Geophysical Research* 42, 6407–
1333 6415. doi:10.1002/ 2015GL064861. 
- 1334 Rashid, R., Eisenhauer, A., Stocchi, P., Liebetrau, V., Fietzke,
1335 J., Rüggeberg, A., Dullo, W.-Ch., 2014. Constraining mid
1336 to late Holocene relative sea-level change in the southern
1337 equatorial Pacific Ocean relative to the Society Islands,
1338 French Polynesia. *Geochemistry, Geophysics, Geosystems*
1339 15, 2601–2615.
- 1340 Richmond, B.M., 1992. Development of atoll islets in the
1341 central Pacific. *Proceedings of the 7th International Coral*
1342 *Reef Symposium, Guam* 2, 185–1194.
- 1343 Salvat, B., 1981. Geomorphology and marine ecology of the
1344 Takapoto Atoll (Tuamotu Archipelago). *Proceedings of*
1345 *the 4th International Coral Reef Symposium, Manila* 1,
1346 503–509.
- 1347 Salvat, B., Richard, G., 1985. Takapoto atoll. *Proceedings of the*
1348 *5th International Coral Reef Congress* 1, 323–378.
- 1349 Scoffin, T.P., 1993. The geological effects of hurricanes on
1350 coral reefs and the interpretation of storm deposits. *Coral*
1351 *Reefs*, 12, 203–221.
- 1352 Scoffin, T.P., McLean, R.F., 1978. Exposed limestones of the
1353 Northern Province of the Great Barrier Reef.
1354 *Philosophical Transactions of the Royal Society of*
1355 *London A* 291, 119–138.

- 1356 Scoffin, T.P., Stoddart, D.R., 1983. Beachrock and inter- tidal
1357 sediments. In: Goudie, A.S., Pye, K. (eds.), Chemical
1358 Sediments and Geomorphology. Academic Press, Inc.,
1359 London, pp. 401–425.
- 1360 Scoffin, T.P., Stoddart, D.R., Tudhope, A.W., Woodroffe, C.D.,
1361 1985. Exposed limestone of Suvarrow Atoll. Proceedings
1362 of the 5th International Coral Reef Congress, Tahiti 3,
1363 137–140.
- 1364 Schofield, J.C., 1977a. Late Holocene sea-level, Gilbert and
1365 Ellice Islands, West Central Pacific Ocean. New-Zealand
1366 Journal of Geology and Geophysics 20, 503–529.
- 1367 Schofield, J.C., 1977b. Effect of Late Holocene sea-level fall on
1368 atoll development. New-Zealand Journal of Geology and
1369 Geophysics 20, 531–536.
- 1370 Shope, J.B., Storlazzi, C.D., Erikson, L.H., 1057 Hegermiller,
1371 C.A., 2016. Changes to extreme wave climates of islands
1372 within the western tropical Pacific throughout the 21st
1373 cen- tury under RCP 4.5 and RCP 8.5, with implications
1374 for island vulnerability and sus- tainability. Global and
1375 Planetary Change 141, 25–38.
- 1376 Sladen, A., Hébert, H., Schindelé, F., Reymond, D., 2007.
1377 Evaluation of far-field tsunami hazard in French Polynesia
1378 based on historical and numerical simulations. Natural
1379 Hazards Earth System Science 7, 195–206.
- 1380 Slangen, A.B.A., Carson, M., Katsman, C.A., van de Wal,
1381 R.S.M., Köhl, A., Vermeersen, L.L.A., Stammer, D.,
1382 2014. Projecting twenty-first century regional sea-level
1383 changes. Climatic Change 124, 317–332.

1384 Stanley, S., 2019, Sea level rise may reactivate growth of some
1385 reef islands. *Eos* 100. doi.org/10.1029/

1386 Stoddart, D.R., 1985. Hurricane effects on coral reefs.
1387 International Coral Reef Congress, Tahiti 3, 350.

1388 Stoddart, D.R., Davies, P.S., Keith, A., 1966. Geomorphology
1389 of Addu Atoll. *Atoll Research Bulletin* 116, 13–41.

1390 Stoddart, D.R., Murphy, F.J., 2018. Attainable standards of
1391 accuracy in the determination of Holocene sea levels in
1392 the central Pacific. *Atoll Research Bulletin* 619, 149–158.

1393 Storlazzi, C.D., Elias, E., Field, M.E., Presto, M.K., 2011.
1394 Numerical modeling of the impact of sea-level rise on
1395 fringing coral reef hydrodynamics and sediment transport.
1396 *Coral Reefs* 30, 83–96.

1397 Storlazzi, C., Elias, E.P.L., Berkowitz, P., 2015. Many atolls
1398 may be uninhabitable within decades due to climate
1399 change. *Scientific Reports* 5, 14546.
1400 doi.org/10.1038/srep14546.

1401 Storlazzi, C.D., Gingerich, S.B., van Dongeren, A., Cheriton,
1402 O.M., Swarzenski, P.W., Quataert, E., Voss, C.I., Field,
1403 D.W., Annamalai, H., Piniak, G.A., McCall, R., 2018.
1404 Most atolls will be uninhabitable by the mid-21st century
1405 because of sea-level rise exacerbating wave-driven
1406 flooding. *Science Advances* 4, eaap9741. doi.org/
1407 10.1126/sciadv.aap9741.

1408 Stuiver, M., Reimer, P.J., 1993. Extended ^{14}C data base and
1409 revised CALIB 3.0 ^{14}C age calibration program. In:
1410 Stuiver, M., Long, A., Kra, R.S. (eds). *Calibration* 193.
1411 *Radiocarbon* 35, 215–230.

1412 Stuiver, M., Reimer, P.J., Reimer, R.W., 2020. CALIB 8.2
1413 [WWW program], <http://calib.org> [accessed date
1414 November 30, 2020].

1415 Toomey, M.R., Donnelly, J.P., Woodruff, J.D., 2013.
1416 Reconstructing mid-late Holocene cyclone variability in
1417 the central Pacific using sedimentary record from Tahaa,
1418 French Polynesia. *Quaternary Science Reviews* 77, 181–
1419 189.

1420 Tracey, J.I., Ladd, H.S., 1974. Quaternary history of Eniwetok
1421 and Bikini atolls, Marshall Islands. *Proceedings of the*
1422 *2nd International Coral Reef Symposium, Australia* 2,
1423 537–550.

1424 Van Dongeren, A.R., Lowe, R., Pomeroy, A., Duong, M.T.,
1425 Roelvink, J.A., Symonds, G., Ranasinghe, R., 2013.
1426 Numerical modeling of low-frequency wave dynamics
1427 over a fringing coral reef. *Coastal Engineering*,
1428 <http://dx.doi.org/10.1016/j.coastaleng.2012.11.004>

1429 Van Woesik, R., Golbuu, Y., Roff, G., 2015. Keep up or drown:
1430 adjustment of western Pacific coral reefs to sea-level rise
1431 in the 21st century. *Royal Society Open Science* 2:
1432 150181. <http://dx.doi.org/10.1098/rsos.150181>

1433 Vercelloni, J., Lique, B., Kennedy, E.V., Gonzalez-Rivero, M.,
1434 Caley, M.J., Peterson, E.E., Puotinen, M., Hoegh-
1435 Guldberg, O., Mengersen, K., 2019. Forecasting
1436 intensifying disturbance effects on coral reefs. *Global*
1437 *Change Biology*. doi: 10.1111/gcb.15059

1438 Vitousek, S., Barnard, P.L., Fletcher, C.H., Frazer, N., Erikson,
1439 L., Storlazzi, C.D., 2017. Doubling of coastal flooding

1440 frequency within decades due to sea-level rise. Scientific
1441 Reports 7: 1399. doi:10.1038/s41598-017-01362-7

1442 Wang, X., Feng, Y., Chan, R., Compo, G.P., Slivinski, L.C., Yu,
1443 B., Wehner, M., Yang, X.-Y., 2020. Cyclone activities as
1444 inferred from the twentieth century reanalysis version 3
1445 (20CRv3) for 1836-2015. EGU General Assembly,
1446 <https://doi.org/10.5194/egusphere-egu2020-5885>

1447 Webb, A.P., Kench, P.S., 2010. The dynamic response of reef
1448 islands to sea-level rise; evidence from multi-decadal
1449 analysis of island change in the central Pacific. Global
1450 and Planetary Change 72, 234–246.

1451 Woodroffe, C.D., McLean, R.F., 1994. Reef Islands of the
1452 Cocos (Keeling) Islands. Atoll Research Bulletin 403, 1–
1453 36.

1454 Woodroffe, C.D., McLean, R.F., Polach, H., Wallensky, E.,
1455 1990a. Sea level and coral atolls: Late Holocene
1456 emergence in the Indian Ocean. Geology 18, 62–66.

1457 Woodroffe, C.D., Stoddart, D.R., Spencer, T., Scoffin, T.P.,
1458 Tudhope, A., 1990b. Holocene emergence in the Cook
1459 Islands, South Pacific. Coral Reefs 9, 31–39.

1460 Woodroffe, C.D., McLean, R.F. Smithers, S.G. and Lawson, E.,
1461 1999. Atoll reef-island formation and response to sea-
1462 level change: West Island, Cocos (Keeling) Islands.
1463 Marine Geology 160, 85–104.

1464 Woodroffe, C.D., Samosorn, B., Hua, Q., Hart, D.E., 2007.
1465 Incremental accretion of a sandy reef island over the past
1466 3000 years indicated by component-specific radiocarbon

1467 dating. *Geophysical Research. Letters* 34, L03602.
1468 <https://doi.org/10.1029/2006GL028875>.

1469 Woodroffe, C.D., and Biribo, N., 2011. Atolls. In: Hopley, D.
1470 (ed) *Encyclopedia of Modern Coral Reefs*. *Encyclopedia*
1471 *of Earth Sciences Series*. Springer, Dordrecht, pp.51–71.

1472 Yamano. H., Kayanne, H., Yamaguchi, T., Kuwahara, Y.,
1473 Yokoki, H., Shimazaki, H., Chikamori, M., 2007. Atoll
1474 island vulnerability to flooding and inundation revealed
1475 by historical reconstruction: Fongafate Islet, Funafuti
1476 Atoll, Tuvalu. *Global and Planetary Change* 57, 407–416.

1477 Yonekura, N., Ishii, T., Saito, Y., Maeda, Y., Matsushima, Y.,
1478 Matsumoto, E., Kayanne, H., 1988. Holocene fringing
1479 reefs and sea-level change in Mangaia Island, southern
1480 Cook Islands. *Palaeogeography, Palaeoclimatology,*
1481 *Palaeoecology* 68, 177–188.

1482 **Figure captions**

1483 **Fig. 1.** Map of French Polynesia, central south Pacific, with
1484 location of the islands cited in the present study.

1485 **Fig. 2.** Google Earth maps of the three atolls (Takapoto,
1486 Takaroa, and Fakarava) under study in the north-western
1487 Tuamotu Archipelago, showing location of the surveyed areas
1488 in each atoll. (a) Takapoto. The boxes labelled as Fig. 3a, b and
1489 Fig. 4a, b and 4c refer to the studied areas presented in the
1490 relevant figures. (b) Takaroa, with location of the studied area
1491 (see Fig. 6). (c) Fakarava, with location of the studied areas

1492 from the atoll rim (See Fig. 7) and lagoonal reef patches A (see
1493 Fig. 8) and B (see Fig. 9) supporting islets.

1494 **Fig. 3.** Google Earth aerial views of Takapoto Atoll (French
1495 Polynesia), showing location of the eight excavation sites from
1496 which conglomerate clasts were collected. (a) Southeastern rim
1497 area. (b) Southwestern rim area. See Fig. 2a for location of both
1498 aerial views.

1499 **Fig. 4.** Google Earth aerial views of Takapoto Atoll (French
1500 Polynesia), showing location of exposed conglomerates
1501 outcrops from which conglomerate clasts were collected. (a)
1502 Southeastern *hoa* system. (b) Northwestern *hoa* system (Takai
1503 locality). (c) Northeastern rim area. See Fig. 2a for location of
1504 aerial views.

1505 **Fig. 5.** Close-up pictures of conglomerate platforms and rubble
1506 sheets, Takapoto Atoll (French Polynesia). (a) Southeastern
1507 *hoa* system. The location of the dated clast samples is
1508 indicated. (b) Northwestern *hoa* system. See Fig. 2 and Fig. 4a
1509 and Fig. 4b respectively for location of the pictures.

1510 **Fig. 6.** Conglomerate platform, northeastern *hoa* system,
1511 Takaroa Atoll (French Polynesia). (a) Google Earth aerial view
1512 of the *hoa* system, showing location of the dated clast samples
1513 at the surface of the exposed conglomerate platform. (b) View
1514 of the conglomerate platform close to the *hoa* system with
1515 location of some dated coral clasts. See Fig. 2b for location of
1516 the studied area.

1517 **Fig. 7.** Conglomerate platforms from the atoll-rim, Fakarava
1518 Atoll (French Polynesia). (a) Google Earth aerial view of the
1519 studied south-eastern rim area, with location of the dated coral
1520 samples. (b) Close-up picture of the two-layer conglomerate
1521 platform located close to the seaward shoreline. (c) Picture of
1522 the exposed two-layer conglomerate platform at the south-
1523 eastern lagoon side. A well-developed marine notch undercuts
1524 the lower conglomerate layer. (d) Picture of the exposed two-
1525 layer conglomerate platform at the south-eastern lagoon side.
1526 The location of the dated clast samples is indicated. See Fig. 2c
1527 for location of the studied area.

1528 **Fig. 8.** Conglomerates platforms from the lagoonal islet-
1529 supporting reef patches, Fakarava Atoll (French Polynesia). (a)
1530 Google Earth aerial view of reef patch A supporting a
1531 vegetated islet. (b) View of the one single-layer conglomerate
1532 platform. (c) Close-up picture of the platform surface showing
1533 embedded coral and molluscan blocks and fragments and
1534 location of one collected sample. The hammer grip is 25 cm
1535 long. See Fig. 2c for location of the studied area.

1536 **Fig. 9.** Conglomerates platforms from the lagoonal islet-
1537 supporting reef patches, Fakarava Atoll (French Polynesia). (a)
1538 Partial view of reef patch E, showing the exposed conglomerate
1539 platform capping the patch. (b) General view of the three-layer
1540 conglomerate platform, 1.30-m thick. (c) Close-up picture of a
1541 conglomerate section showing the stacked arrangement of the

1542 three distinct layers. The location of the dated clast samples is
1543 indicated. See Fig. 2c for location of the studied area.

1544 **Fig. 10.** Age distribution graphs of coral clasts from
1545 conglomerate platforms: relative frequency and percentage of
1546 clasts per 1,000-yr age range. (a) 53 U/Th-dated samples from
1547 conglomerate clasts collected at Takapoto, Takarua and
1548 Fakarava Atolls. (b) 75 samples including 57 U/Th-dated
1549 samples from Takapoto, Takarua and Fakarava Atolls and 18
1550 radiocarbon-dated samples from conglomerates collected on
1551 nine Tuamotu Atolls (Takapoto, Mataiva, Rangiroa, Arutua,
1552 Apataki, Marokau, Hao, Pukarua, Nukutavake). (c) 48 U/Th-
1553 dated samples from conglomerates in eight French Polynesian
1554 archipelagoes (Bora Bora, Moorea, Rangiroa, Tikehau,
1555 Fakarava, Hao, Makemo, Gambier). Dataset from Hallmann et
1556 al., 2020. (d) 145 radiometrically dated samples including 107
1557 U/Th-dated and 37 radiocarbon-dated. Sources for U/Th ages:
1558 57 from Montaggioni et al. (2018, 2019a) and the present
1559 study; three from Rashid et al. (2014) and 48 from Hallmann et
1560 al. (2020). Is also indicated the cyclone activity over the past
1561 3,000 years at Tahaa Island, Society archipelago. Cyclogenesis
1562 is based on grain-size analysis, i.e. percentage of coarse
1563 fraction > 250 μm , in a core from lagoonal sediments (Toomey
1564 et al., 2013; Bramante et al., 2020b).

1565 The three histograms are left-skewed, indicating higher
1566 frequency of ages ranging between 3,000 and 1,000 yr BP. The

1567 four samples (SAT 21, 23, 24, 26) collected from a modern
1568 rubble sheet, regarded as conglomerates in the making, in the
1569 northwest of Takapoto, are included in the compiled data.

1570 **Fig. 11.** Lateral age distribution of conglomerate clasts in order
1571 of distance from adjacent reef front lines at Takapoto, Takaroa,
1572 and Fakarava Atolls. The slope of the dotted lines reflects
1573 increasing age trends lagoonwards. The lines are fitted based
1574 on the mean values of youngest and oldest U/Th dated coral
1575 samples. SAT, BAT = field sample codes (see [Supplementary](#)
1576 [material](#)).

1577 **Fig. 12.** Reconstructed history of conglomerate deposition and
1578 cementation, atoll-island accretion in the regional context of
1579 sea-level change over the last 6,000 years. The mean sea level
1580 curve is simplified from Hallmann et al., (2020, Figure 11).

1581 **Fig. 13.** Conceptual model of reef conglomerate deposition in
1582 subsiding northwestern Tuamotu Atolls over the 6,000–1,000
1583 yr interval. (a) About 6,000 years ago: atoll-rim surfaces were
1584 about 5–6 m below sea level. Due to storm surges, most clasts
1585 were moved backwards across reef tops, this resulting in the
1586 building of detrital talus. (b) 4,000 years ago: rim surfaces were
1587 close to sea level. Rubble sheets started to extend over inner
1588 reef rim surfaces while a significant amount of coral detritus
1589 has been deposited along the lagoonal slopes (c) Between 3,000
1590 and 1,000 yr BP, coral-clast production was optimal. As rubble
1591 sheets have growing and expanding rapidly seawards step by

1592 step, lithification has occurred together with clast deposition.

1593 Discrepancy in lithification rates between conglomerates and

1594 islets results from their respective development in different

1595 diagenetic environments, marine *versus* subaerial.

1596 **Table 1.** List of radiometrically dated coral samples from

1597 conglomerate platforms, French Polynesia, ranked by islands,

1598 radiometric dating methods and published references.

1599 References: a. Montaggioni et al. (2018, 2019); the present

1600 study, see Supplementary data. b. Hallman et al. (2020). c.

1601 Rashid et al. (2014). d. Montaggioni and Pirazzoli (1984). e.

1602 Pirazzoli and Montaggioni (1986). f. Pirazzoli and Montaggioni

1603 (1988b. g. Pirazzoli et al. (1988).

1604 **Table 2.** List of calibrated ^{14}C ages from conglomerate clasts,

1605 Tuamotu atolls (French Polynesia). Calibrations performed

1606 from the conventional age datasets: Takapoto (Pirazzoli and

1607 Montaggioni, 1984); Mataiva, Rangiroa, Arutua, Apataki

1608 (Pirazzoli and Montaggioni, 1986); Marokau, Hao, Pukarua,

1609 Nukutavake (Pirazzoli et al., 1988).

1610 Sampling was conducted along vertical sections at different

1611 elevations relative to present mean sea level (pmsl). Elevations

1612 were measured using manual levelling and given at ± 0.05 to

1613 0.30 m relative to pmsl. A correction by subtracting 140 ± 20

1614 years to conventional ^{14}C ages were applied to eliminate age

1615 reservoir effects. The standard deviations (errors \pm) on the

1616 calibrated ages are given in 1 sigma. Readers are advised that

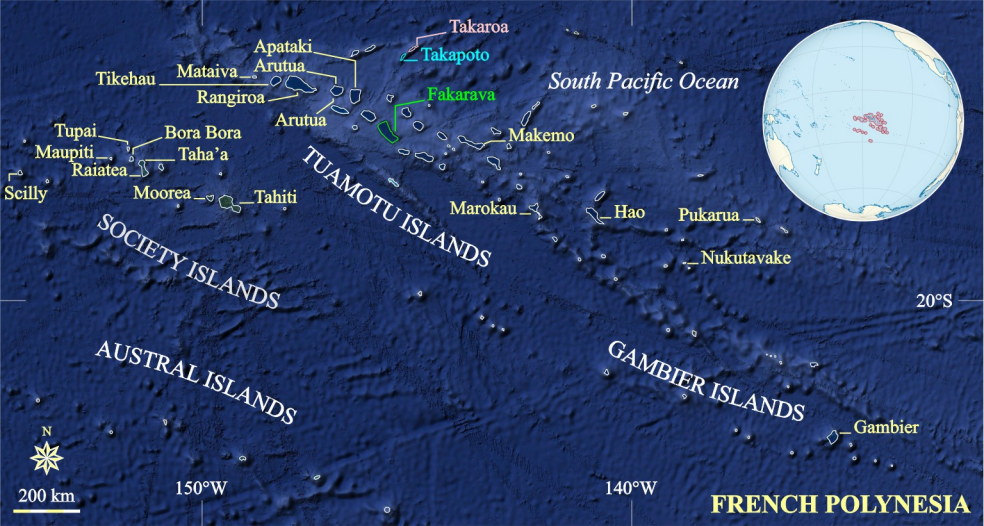
1617 calendars ages and ranges are rounded to the nearest 10 years
1618 for samples with standard deviation in the radiocarbon age
1619 greater than 50 years. The age of sample Hv-13011 cannot
1620 calibrate due to nuclear testing ^{14}C .

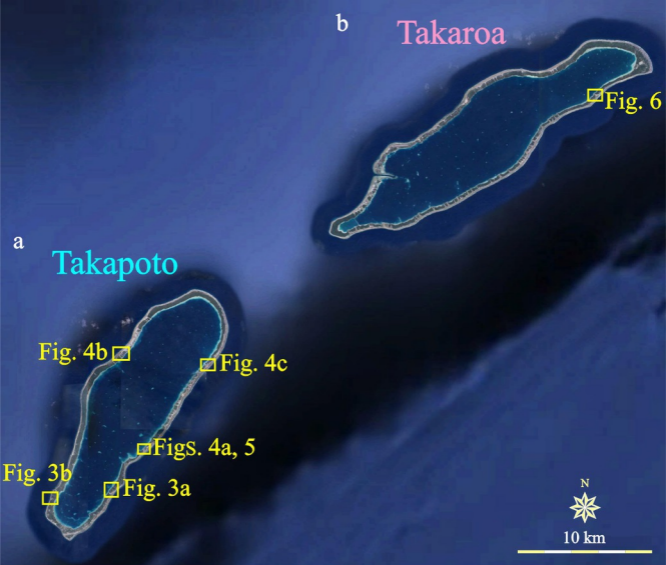
1621 **Table 3.** List of calibrated ^{14}C ages from conglomerate clasts,
1622 Society Islands (French Polynesia). The calibrations were
1623 performed from the conventional ^{14}C age dataset published by
1624 Pirazzoli (1985). See the caption of Table 2 for more details on
1625 the field and dating the procedures used.

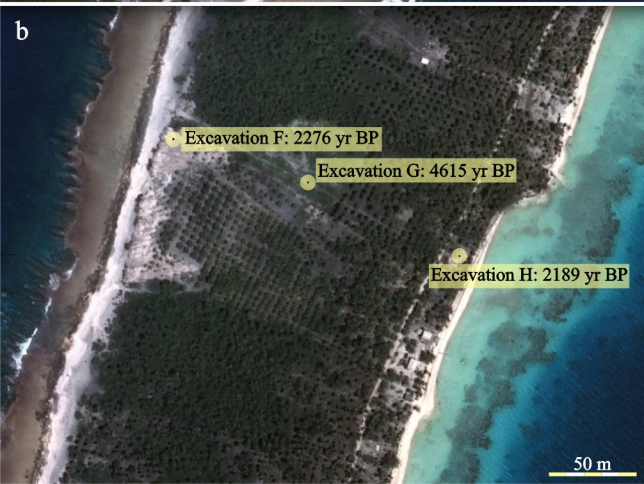
1626 **Supplementary data.** List of uranium-thorium ages of coral
1627 clasts collected from Takapoto, Takaroa and Fakarava Atolls,
1628 northwestern Tuamotu, French Polynesia. Are given
1629 successively laboratory code numbers, field sample numbers
1630 (BAT, SAT, FAK), uranium and thorium concentrations,
1631 isotopic composition with statistical errors – two standard
1632 deviation of the mean – and ages expressed in calendar years
1633 BP (Before Present) relative to the year of sample analysis.

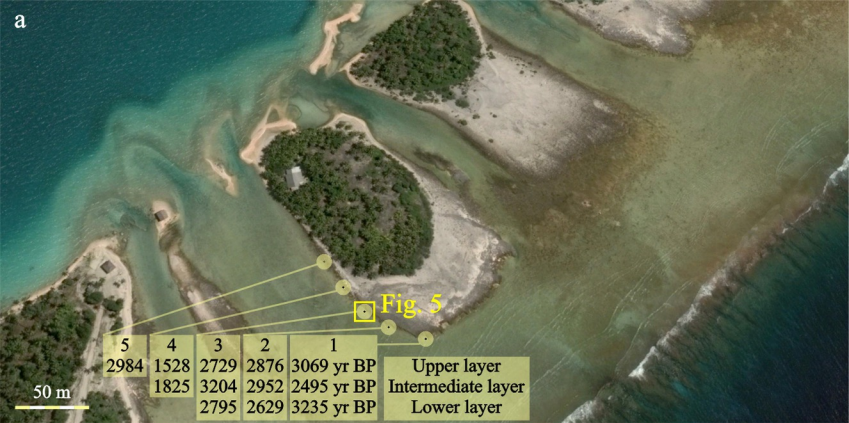
1634 The samples marked by an asterisk within the *laboratory code*
1635 column were analyzed by Anton Eisenhauer at the GEOMAR
1636 Institute, Kiel, Germany. All the other samples were analyzed
1637 by Edwige Pons-Branchu at Laboratoire des sciences du climat
1638 et de l'environnement, Gif-sur-Yvette, France. More details on
1639 the analytical procedure – chemistry and MC-ICPMS
1640 analysis – can be found in Pons-Branchu et al. (2014). At
1641 GEOMAR, determination of uranium and thorium isotope

1642 ratios ($^{230}\text{Th}/^{234}\text{U}$) used multi-ion-counting inductively coupled
1643 plasma mass spectroscopy (MC-ICP-MS) following the method
1644 of Fietzke et al. (2005). The ages were calculated using the
1645 half-lives published by Cheng et al. (2000). For isotope dilution
1646 measurements, a combined $^{233}\text{U}/^{236}\text{U}/^{229}\text{Th}$ spike was used with
1647 stock solutions calibrated for concentration using NISTSRM
1648 3164 (U) and NIST-SRM 3159 (Th) as combi-spike, calibrated
1649 against CRM-145 uranium standard solution – formerly known
1650 as NBL-112A – for uranium isotope composition and against a
1651 secular equilibrium standard – HU-1, uranium ore solution –
1652 for the precise determination of $^{230}\text{Th}/^{234}\text{U}$ activity ratios – see
1653 Montaggioni et al. (2018)for more details on the analytical.
1654 The vertical error range for elevations is estimated at a
1655 maximum value of ± 0.30 m relative to present mean sea level.
1656









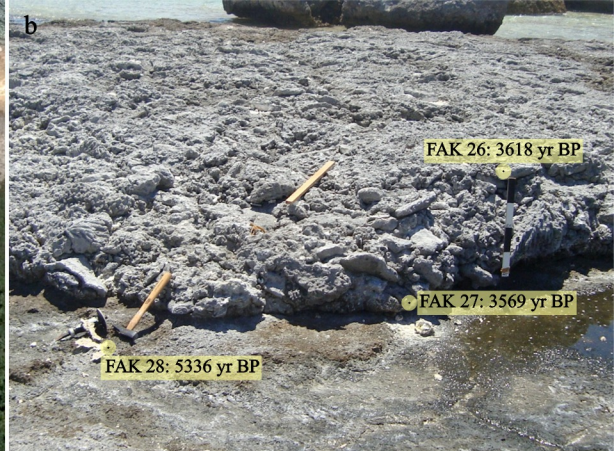
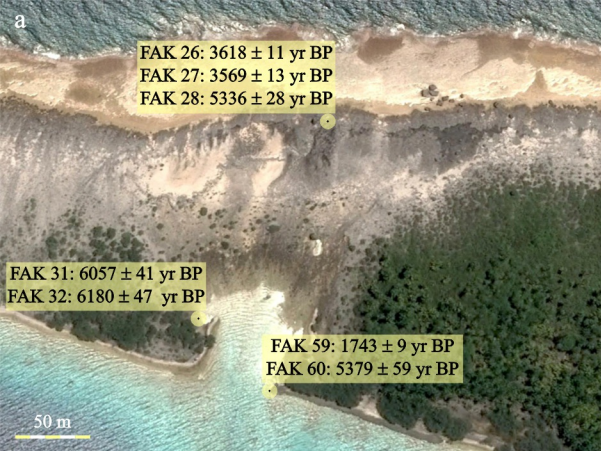


a



b





a

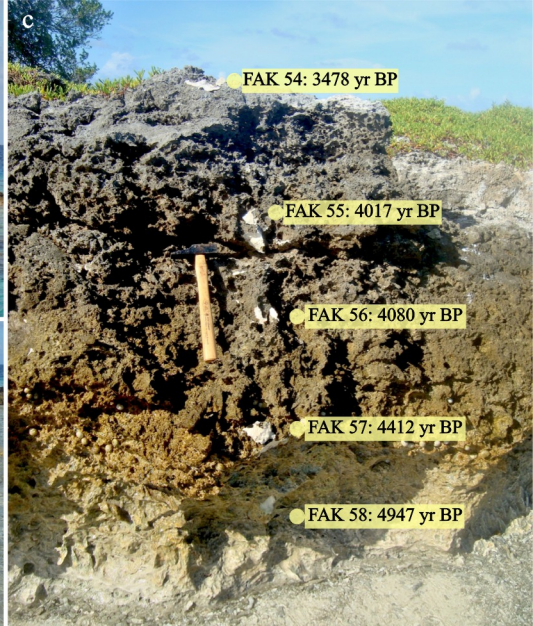
Fig. 8b, c □

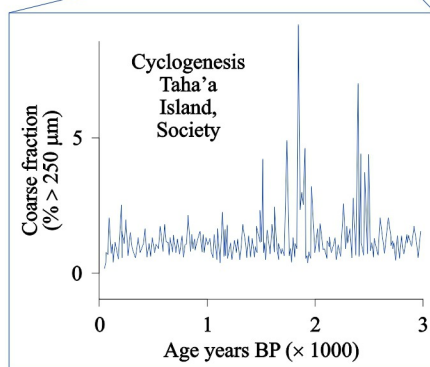
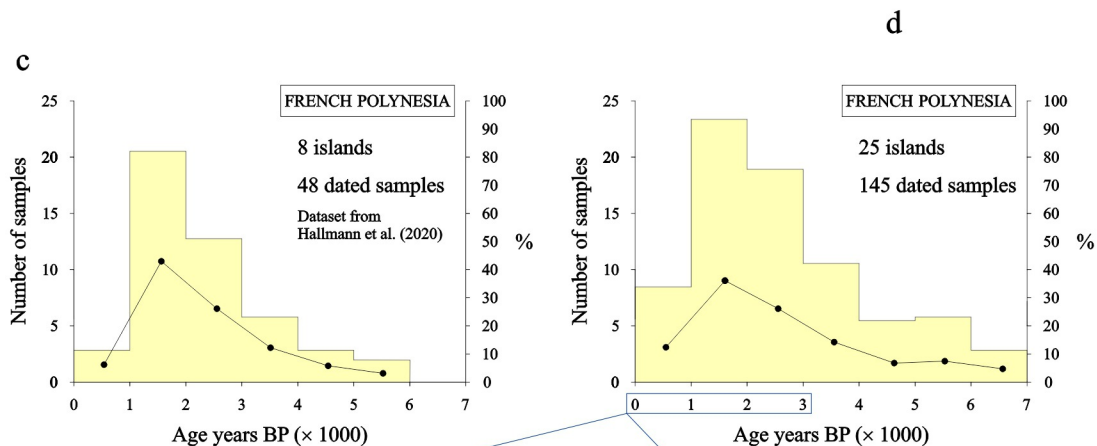
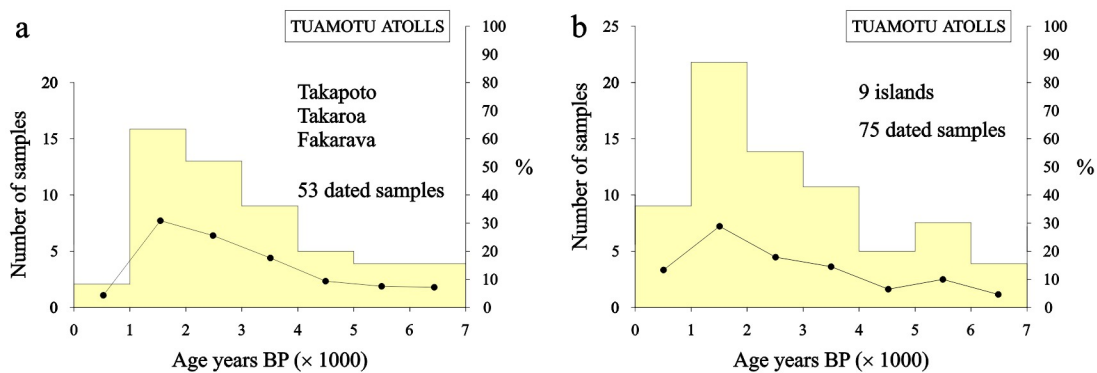
50 m

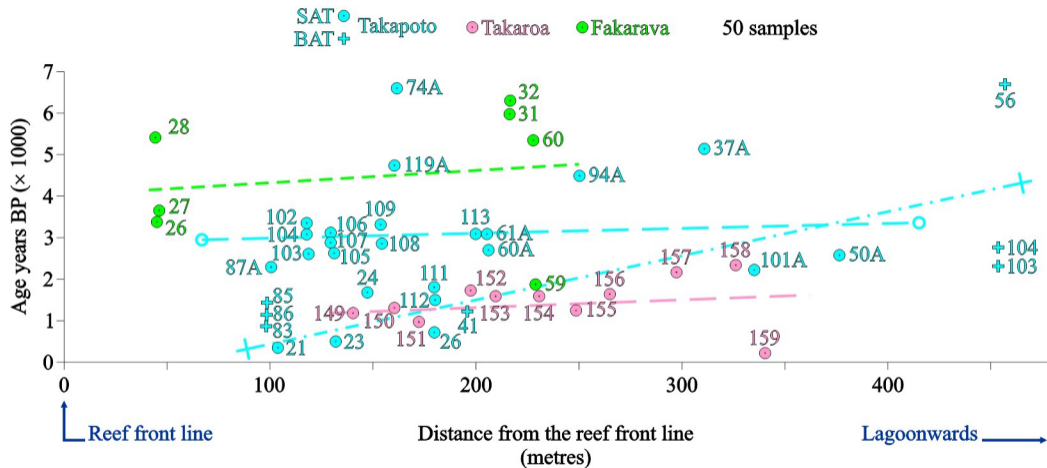
b

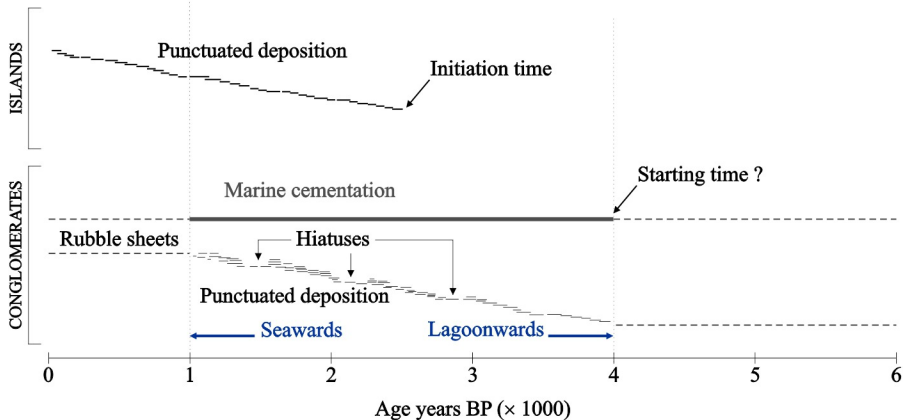
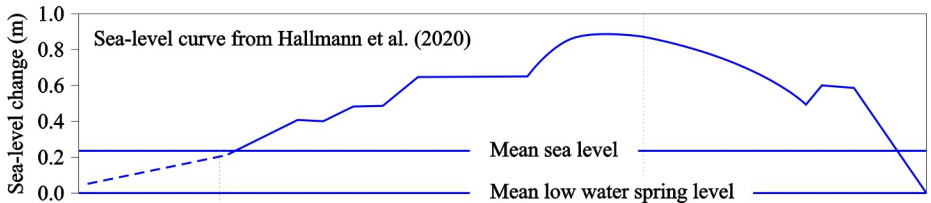
FAK 34: 1220 yr BP
FAK 35: 629 yr BP

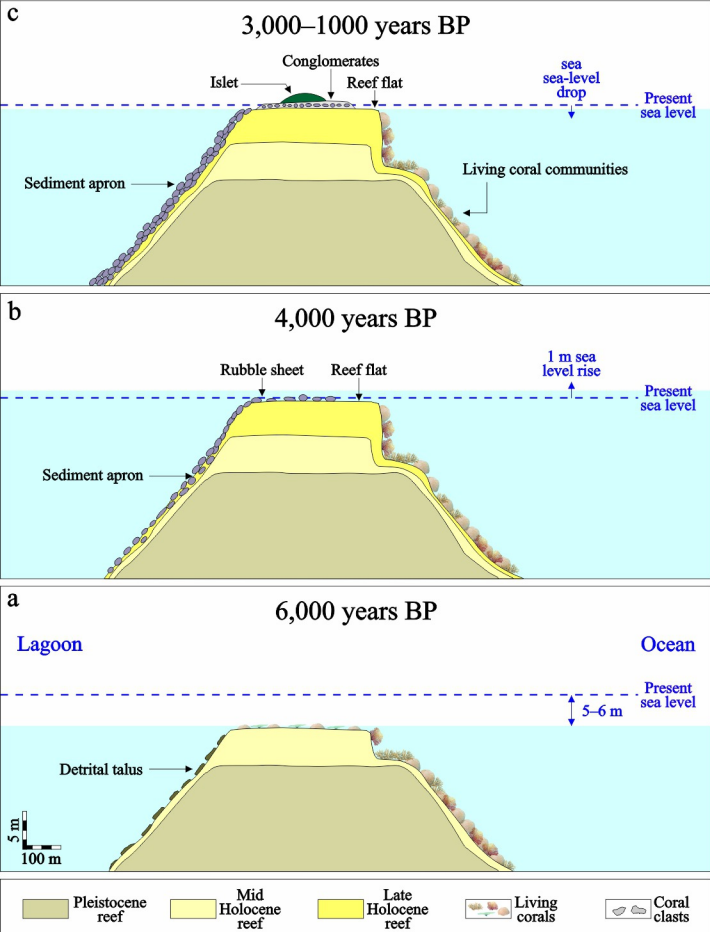
c











	Uranium-thorium dating		Calibrated ¹⁴ C dating		Total
References	a	b	c	d,e,f,g	
Islands					
Tuamotu					
Takapoto	31			3	
Takaroa	12				
Mataiva				3	
Tikehau		8			
Rangiroa		9		3	
Fakarava	14	5			
Arutua				2	
Apataki				3	
Marokau				1	
Hao		4		1	
Pukarua				1	
Nukutavake				1	
Makemo		2			
Society					
Scilly				2	
Maupiti				1	
Tupai				2	
Bora Bora		9		2	
Raiatea				1	
Moorea		8	3	7	
Tahiti				4	
Gambier					
Gambier		3			
Total	57	48	3	37	145

Field sample numbers	Laboratory numbers	Locality – Islands Sites	Latitude south – Longitude west	Elevation (above pmsl)	Conventional ¹⁴ C ages	calibrated (calendar) ages (yr BP)
TK60	GaK-9976	Takapoto Tavake	14°36'10"–145°09'26"	0.55	5,020 ± 140	5,310 + 188 / – 185
TA-10	Hv-12275	Takapoto Orapa	14°39'48"–145°12'35"	0.30	1,560 ± 70	1,095 + 93 / – 109
TA-11	Hv-12276	Takapoto Orapa	14°39'48"–145°12'35"	0.45	1,320 ± 80	844 + 92 / – 118
MV-2	GaK-9970	Mataiva south reef	14°54'32"–148°40'41"	0.20	5,420 ± 110	5,751 + 130 / – 141
MV-3A	Gak-9971	Mataiva Hitirari	14°54'10"–148°41'33"	0.20	5,230 ± 140	5,547 + 167 / – 176
MV-3B	GaK-9972	Mataiva Hitari	14°54'10"–148°41'33"	0.60	3,470 ± 120	3,343 + 158 / – 170
RA-2	Hv-12282	Rangiroa Tepaetia	15°56'03"–147°43'12"	0.40	705 ± 65	309 + 116 / – 80
	LJ-1372	Rangiroa Tiputa	14°59'04"–147°36'25"	–0.30	4,900 ± 300	5,147 + 389 / – 336
RA-14	Hv-12283	Rangiroa Motu Paio	15°01'13"–137°45'25"	0.50	2,775 ± 65	2,511 + 115 / – 122
AR-1	Hv-12280	Arutua Rautini	15°22'04"–146°37'16"	0.60	1,380 ± 70	905 + 92 / – 112
AR-3	Hv-12281	Arutua Rautini	15°22'04"–146°37'16"	0.40	1,565 ± 65	1,100 + 92 / – 105
AP-6	Hv-12278	Apataki Teavatika	15°31'24"–146°25'40"	0.70	3,135 ± 65	2,931 + 108 / – 115
AP-7	Hv-12279	Apataki Teavatika	15°31'24"–146°25'40"	0.40	2,990 ± 130	2,766 + 186 / – 174
AP-4	Hv-12277	Apataki Hutihuti	15°34'29"–146°24'55"	0.45	1,580 ± 70	1,115 + 110 / – 92
3MA1	Hv-13011	Marokau north--west	18°00'33"–141°22'58"	0.30	210 ± 70	
3B	Gif-1667	Hao, north- north-east	18°04'02"–140°57'05"	1.30	3,300 ± 100	3,135 + 153 / – 144
3PU7	Hv-13021	Pukarua north-west	18°17'00"–137°03'47"	0.60	3,875 ± 70	3,850 + 116 / – 130
3NU3	Hv-13009	Nukutavake north-west	19°16'54"–138°48'06"	2.0	2,315 ± 65	1,927 + 110 / – 110

Field sample numbers	Laboratory numbers	Locality – Islands Sites	Latitude south – Longitude west	Elevation (above pmsl)	Conventional ¹⁴ C ages	Calibrated (calendar) ages (yr BP)
3Sci1	Gif-6414	Scilly, north-east	16°30'23"–154°38'44"	0.50	2,640 ± 60	2,337 + 113 / – 120
3Sci2	Gif-6415	Scilly, south-east	16°33'52"–154°37'17"	1.2	390 ± 60	
2MA13	Gif-6563	Maupiti, Motu Paeao	16°25'05"–152°15'40"	0.60–0.65	2,200 ± 60	1,786 + 106 / – 98
3TP10	Gif-6505	Tupai hoa east	16°15'33"–151°48'05"	0.30	2,910 ± 60	2,668 + 96 / – 109
3TP11	Gif-6506	Tupai hoa east	16°15'33"–151°48'05"	0.50	2,780 ± 60	2,517 + 117 / – 114
2BB2	Gif-6561	Bora Bora West Motu Mute	16°26'29"–151°45'44"	0.40	980 ± 50	548 + 70 / – 59
2BB4	Gif-6562	Bora Bora West Motu Mute	16°26'29"–151°45'44"	0.80	2,500 ± 60	2,161 + 120 / – 93
2RAI8	Gif-6097	Raiatea Motu Tetaro	16°44'30"–151°25'11"	0.20	3,880 ± 80	3,856 + 124 / – 143
MO84	GaK-9974	Moorea Aroa	17°28'38"–149°46'02"	0.60	6,070 ± 130	6,453 + 151 / – 160
MO112	GaK-9975	Moorea Motu Ahi	17°33'09"–149°46'32"	0.55	3,340 ± 120	3,183 + 169 / – 161
MO6	Gif-6099	Moorea Motu Ahi	17°33'09"–149°46'32"	0.35	2,320 ± 60	1,933 + 103 / – 108
MO5	Gif-6098	Moorea Motu Ahi	17°33'09"–149°46'32"	0.10	2,690 ± 70	2,407 + 127 / – 118
MO7	Gif-6100	Moorea Motu Ahi	17°33'09"–149°46'32"	0.75	2,670 ± 60	2,38 + 118 / – 107
	Gif-3881	Moorea Temae	17°28'24"–149°46'28"	1.60	1,370 ± 100	896 + 120 / – 129
	Gif-3880	Moorea Temae	17°28'24"–149°46'28"	0.80	2,280 ± 100	1,885 + 135 / – 152
2TH1	Gif-6101	Tahiti-Nui PK12 west	17°37'00":149°37'02"	0.30	2,610 ± 60	2,294 + 97 / – 125
TH1	GaK-10711	Tahiti-Nui Pointe Tataa	17°34'28"–149°37'14"	0.50	5,360 ± 130	5,689 + 172 / – 140
2TH3	Gif-6102	Tahiti-Nui Pointe Honu	17°31'01"–149°30'38"	0.20	3,660 ± 60	3,572 + 101 / – 109
2TH5	Gif-6104	Tahiti-lti Taharoa	17°44'34"–149°12'13"	0.15	2,850 ± 60	2,594 + 113 / – 95